Kasai, S., Shiku, H., Torisawa, Y.S., Nagamine, K., Yasukawa, T., Watanabe, T., Matsue, T., 2006. Anal. Chim. Acta 566, 55–59.
Li, Y.B., Zhu, H., Trush, M.A., 1999. Biochim. Biophys. Acta 1428 (1), 1–12.
Linke, B., Kerner, W., Kiwit, M., Pishko, M., Heller, A., 1994. Biosens. Bioelectron. 9, 151–158.
Liu, X.P., Zweier, J.L., 2001. Free Radic. Biol. Med. 31, 894–901.
Lundqvist, H., Dahlgren, C., 1996. Free Radic. Biol. Med. 20, 785–792.
Matsuura, H., Sato, Y., Niwa, O., Mizutani, F., 2005. Anal. Chem. 77, 4235–4240.
Mizutani, F., Ohta, E., Mie, Y., Niwa, O., Yasukawa, T., 2008. Sens. Actuators B Chem. 135, 304–308.
Muranaka, S., Fujita, H., Fujiwara, T., Ogino, T., Sato, E.F., Akiyama, J., Imada, I., Inoue, M., Utsumi, K., 2005. Antioxid. Redox Signal. 7, 1367–1376.
Nakajima, K., Yamagiwa, T., Hirano, A., Sugawara, M., 2003. Anal. Sci. 19, 55–60.
Radi, R., Cosgrove, T.P., Beckman, J.S., Freeman, B.A., 1993. Biochem. J. 290, 51–57.
Rossi, F., 1986. Biochim. Biophys. Acta 853, 65–89.
Ruzgas, T., Csoregi, E., Emneus, J., Gorton, L., MarkoVarga, G., 1996. Anal. Chim. Acta 330, 123–138.
Shleev, S., Wettero, J., Magnusson, K.E., Ruzgas, T., 2008. Cell Biol. Int. 32, 1486–1496.
Stefanska, J., Pawliczak, R., 2008. Mediators Inflamm. 2008, 1–10.
Umegaki, K., Fenech, M., 2000. Mutagenesis 15, 261–269.
Vreeke, M., Maidan, R., Heller, A., 1992. Anal. Chem. 64, 3084–3090.

Electrochemical characterization of enzymatic activity of yeast cells entrapped in a poly(dimethylsiloxane) microwell on the basis of limited diffusion system

Hitoshi Shiku,*[a] Shun Goto,[a] Sungbong Jung,[a] Kuniaki Nagamine,[a] Masahiro Koide,[b] Tomosato Itayama,[b] Tomoyuki Yasukawa[c] and Tomokazu Matsue*[a]

Received 19th May 2008, Accepted 2nd September 2008
First published as an Advance Article on the web 20th October 2008
DOI: 10.1039/b808428a

A highly sensitive and quantitative analysis was performed using a poly(dimethylsiloxane) (PDMS) microwell array in a scanning electrochemical microscopy setup. A microelectrode with a relatively large seal radius was used to cover the top of the cylindrical PDMS microwell (96 pL). The voltammogram for 4 mM ferrocyanide resulted in a charge value of 38 nC, suggesting that almost 100% of the reductant in the microwell was converted to the oxidation current. When genetically modified yeast cells were entrapped in the microwell, the accumulation of *p*-aminophenol (PAP) produced by expressing β-galactosidase (βGAL) was successfully observed.

1. Introduction

Analytical chemistry within small volumes has shown significant impacts to explore new research fields including single-cell analysis[1–6] and single molecule dynamics.[7,8] Various micro- and nanostructures were constructed and combined with highly sensitive detection systems based on optical and electric amplifiers for the purpose of simplifying sample preparation, shortening the time per assay, and elevating the throughput of the analysis. Among these micro- and nanostructures, poly(dimethylsiloxane) (PDMS) microchamber arrays[7,9] or microchannels[8,10–12] are probably the most simple and flexible devices that can be used as lab-on-a-chip devices.

The electrochemical measurement system is also possible to realize parallel and rapid assays with a small-volume microwell array.[13] However, electrochemical studies of small-volume samples require at least two electrodes to maintain the entire electric circuit connected during the measurements.[14–23] Therefore, the electrode must be designed inside the microchamber[14–19] or inserted into the small space under a micromanipulator operation.[20–23] In the experimental setup based on scanning electrochemical microscopy (SECM),[24,25] however, it is relatively easy to form a confined ultra-small volume.[26–28] The electrochemical behavior of the microelectrode observed in the microchamber is drastically different from that observed when the electrode is placed in the bulk solution. In the present study, we combined the SECM technology with the PDMS cylindrical microwell array to quantitatively evaluate the enzymatic activity of recombinant yeast cells expressing β-galactosidase (βGAL). As a model system, a yeast-two-hybrid strain was selected because it is widely used not only for screening protein–protein interactions but also for detecting environmental pollutants.[5,6,29–36] Schwartz–Mittelman *et al.* demonstrated the electrochemical evaluation of the estradiol activities of various compounds by using human estrogen receptor-alpha.[31–32]

The accumulated product from the yeast cells in the microwell is converted to electric charge. The enzymatic activity of the yeast cells in the confined system is quantitatively analyzed and compared with that in the open system based on the spherical diffusion theory. We find that the cellular activity is strongly affected by the designs of the microchamber and detection system. The confined PDMS microwell system allows the accumulation of the product, and therefore, is advantageous for highly sensitive analyses. However, we must be careful to discuss the enzymatic activity and mass transfer rate in small volume analysis because these parameters might change depending on the environmental conditions.

2. Materials and methods

2.1 Reagents

The (100) silicon monocrystal wafer (thickness: 230 μm, optically polished on both sides) was purchased from SUMO Co., Tokyo, Japan. The negative photoresist, SU-8-3050, was purchased from Microchem Co. USA. PDMS (Sylgard 184) was purchased from Dow Corning, Co. USA. 17β-Estradiol was purchased from Sigma, USA. *p*-Aminophenyl-β-D-galactopyranoside (PAPG) was purchased from Tokyo Chemical Industry Co., Ltd., Japan. Triton X-100 was purchased from Polysciences, Inc., USA. Dimethyl sulfoxide (DMSO) and *p*-aminophenol (PAP) were purchased from Wako Pure Chemicals, Japan. All the solutions were prepared using distilled and deionized water purchased from Direct-Q (Millipore, USA).

2.2 Fabrication of the PDMS microwell array

The PDMS microwell array was fabricated by curing the prepolymer on the (100) Si substrate with a master. The master

[a]*Graduate School of Environmental Studies, Tohoku University, 6-6-11, Aramaki-Aoba, Sendai 980-8579, Japan. E-mail: shiku@bioinfo.che.tohoku.ac.jp; matsue@bioinfo.che.tohoku.ac.jp*
[b]*Environmental Chemistry Division, National Institute for Environmental Studies, 16-2 Onogawa, Tsukuba 305-8506, Japan*
[c]*Graduate School of Material Science, University of Hyogo, Hyogo, Japan*

was photolithographically patterned using the negative photoresist (SU-8 3050). A 10 : 1 mixture of the silicon elastomer and the curing agent was poured on the master and left at 80 °C for 1 h for curing the prepolymer. The PDMS replica was then peeled from the substrate. The diameter and depth of the PDMS microwell were both 50 μm.

2.3 Yeast strain and growth conditions

The yeast strain used in the present study was *Saccharomyces cerevisiae* Y190, donated by Dr Fujio Shiraishi from the National Institute for Environmental Studies. The expression plasmid contains the human estrogen receptor α (hERα),[31–35] instead of the medaka estrogen receptor α (medERα: *Oryzia latipes*),[29] fused with GAL4 DBD (binding domain). The plasmid containing coactivator TIF2 fused with the GAL4 activation domain (GAL4 AD) was also introduced into the yeast cells carrying the β-galactosidase reporter gene.[33,34] The cells were preincubated for 24 h at 30 °C with shaking at 100 rpm in a modified Sabouraud dextrose (SD) medium (without tryptophan and leucine).

The cell suspension (60 μL) was then mixed with the medium (60 μL) containing 10 nM 17β-estradiol and 2.0% (v/v) DMSO, and incubated for 4 h at 30 °C with shaking at 100 rpm to induce the β-galactosidase expression. The medium was exchanged to a 80 μL of Z-buffer (60.0 mM $Na_2HPO_4 \cdot 12H_2O$, 39.7 mM $NaH_2PO_4 \cdot 2H_2O$, 10.0 mM KCl, 10.0 mM $MgSO_4 \cdot 7H_2O$; pH 7.0) including 0.3% (v/v) Triton X-100, a nonionic surfactant to incubate for 1 h at 30 °C with shaking at 100 rpm (final concentration of the yeast cells was 1×10^7 cells mL^{-1}).

2.4 Electrochemical detection of β-galactosidase activity in yeast cells

The PDMS microwell array was irradiated with O_2 plasma at 100 W for 1 min in order to make the surface of the well hydrophilic. Generally, the O_2 plasma treated PDMS surface maintains the sufficient hydrophilic nature for 1 h to smoothly introduce aqueous solutions within the microwell array. Under aqueous solution, however, the hydrophilic nature of the O_2 treated PDMS surface is maintained for at least 12 h.The yeast cell suspension (100 μL) was first dispensed on the PDMS microwell array and stabilized for 10 min. Then, the suspension was withdrawn using a filter paper to remove the excess yeast cells present on the outer surface of the microwell. The liquid and yeast cells remained the inside the PDMS wells only. Secondary, the measuring solution was further poured on the PDMS microwell array gently. For the electrochemical measurements, the PDMS microwell array containing the yeast cells was carefully soaked in the Z-buffer solution containing 7.4 mM PAPG and 0.3% Triton X-100. The concentration of Triton X-100 in the measuring solution was determined to optimize the activity of the yeast cells. The mass-transfer of PAPG and PAP through the cellular membranes was sufficiently promoted, but βGAL still remained in the yeast cells. In this study, the number of cells in the PDMS microwell was controlled to be less than 150 so that the yeast cells remain at the bottom (50 μm ∅) of the cylindrical PDMS microwell at monolayer level. The exact number of cells in the well was manually counted from the photograph recorded for each microwell in which the electrochemical measurement was performed.

The electrochemical measurement was carried out using an SECM system including a potentiostat (HA1010mM8; Hokuto Denko Corp., Tokyo, Japan), an inverted microscope (Nikon diaphot T200), and a motor-driven XYZ stage (Chuo-Seiki M9103). An Ag/AgCl-saturated KCl electrode was used as the reference/counter electrode. A Pt-microelectrode (radius: 10 μm; radius of the tip including the insulator part: 85 μm) was used as the working electrode. The β-galactosidase (βGAL) activity expressed in the yeast cells was monitored by detecting the oxidation current for PAP, a product of the enzyme-catalyzed hydrolysis of PAPG inside the trapped cells.[29–32,37–40] The electrochemical experiment was performed on a 4–6 cm^2 -piece of the PDMS microwell array sheet set in a disposable 60 mm-diameter culture dish. The Ag/AgCl reference electrode was set on the PDMS microwell array sheet. The distance between the working and the reference electrode was about 10–20 mm. In the case that the glass seal part of the working electrode completely covers the PDMS microwell, electrochemical measurement is not available because current does not flow. However, we have recognized that there is an electric connection due to leakage of the ionic flow between the working and the reference electrodes even when reactant within the microwell was consumed almost 100%.

3. Results and discussion

Fig. 1(a) shows the schematic illustration of the experimental setup. The top opening of the PDMS cylindrical microwell is covered with the disk plane of a working microelectrode tip to accumulate PAP produced by βGAL in the yeast cells. The time period between the covering of the PDMS microwell with the microelectrode tip and the application of the potential was defined as the accumulation time, t_{accu}. As t_{accu} increases, the concentration of PAP in the microwell also increases. After maintaining the tip potential at 0.0 V for t_{accu}, the potential was stepped to +0.3 V to oxidize PAP accumulated in the microwell. The product of the PAP oxidation is quinone imine (QI). Fig. 1(b) shows an optical micrograph of the PDMS microwell array. The height of the SU-8 mold of the PDMS microwell was 50 ± 1 μm measured with a surface profiler. The diameter of the microwell was 50 ± 1.3 μm under the optical microscopic observation.

Prior to the measurements using the yeast cells, the electrochemical behavior in the confined microwell was characterized by cyclic voltammetry. Fig. 2 shows the cyclic voltammograms (CVs) of 4.0 mM $K_4Fe(CN)_6$/0.1 M KCl in the PDMS microwell. CVs shown in the present study were performed at scan rate of 20 mV s^{-1}. The microelectrode was positioned at various heights (z) from the upper surface of the PDMS microwell (+300 to −100 μm). The point at $z = 0$ defines the position where the tip touches the upper surface of the PDMS microwell. The negative z value does not reflect the actual z-position of the tip, but indicates that the microelectrode pushes down the top of the PDMS microwell. According to the spherical diffusion theory, when the microelectrode tip is sufficiently far from the upper surface of the PDMS microwell ($z = +300$ μm), the CV has a typical sigmoidal shape, and the oxidation current for $Fe(CN)_6^{4-}$ reaches the

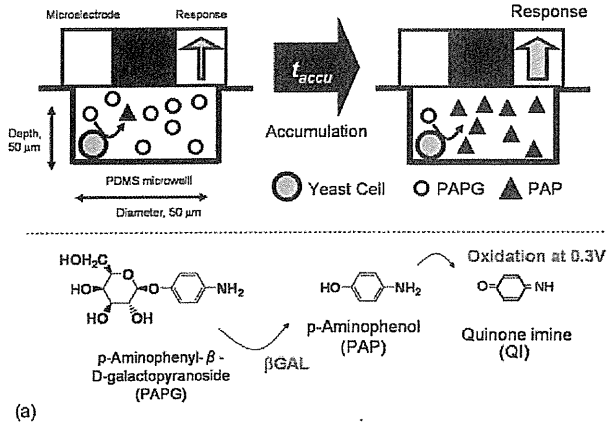

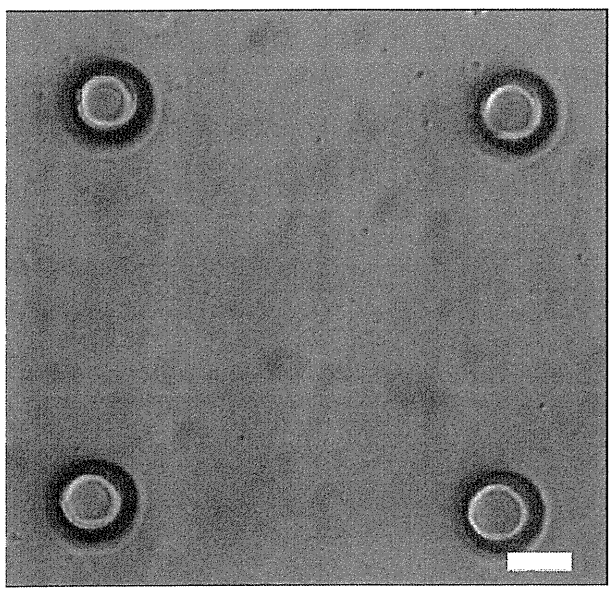

(b)

Fig. 1 (a) Schematic illustration of the experimental setup. The top of the PDMS cylindrical microwell (diameter: 50 μm; depth: 50 μm) is covered with the disk plane of a working microelectrode tip to accumulate the PAP produced by the βGAL in the yeast cells. The accumulation time was defined as t_{accu}. After maintaining the tip potential at 0 V for t_{accu}, the potential was stepped to +0.3 V to oxidize the PAP accumulated in the microwell. Schemes of the enzymatic and electrochemical reaction were also showen. (b) Photograph of the PDMS micriowell array. Bar, 50 μm.

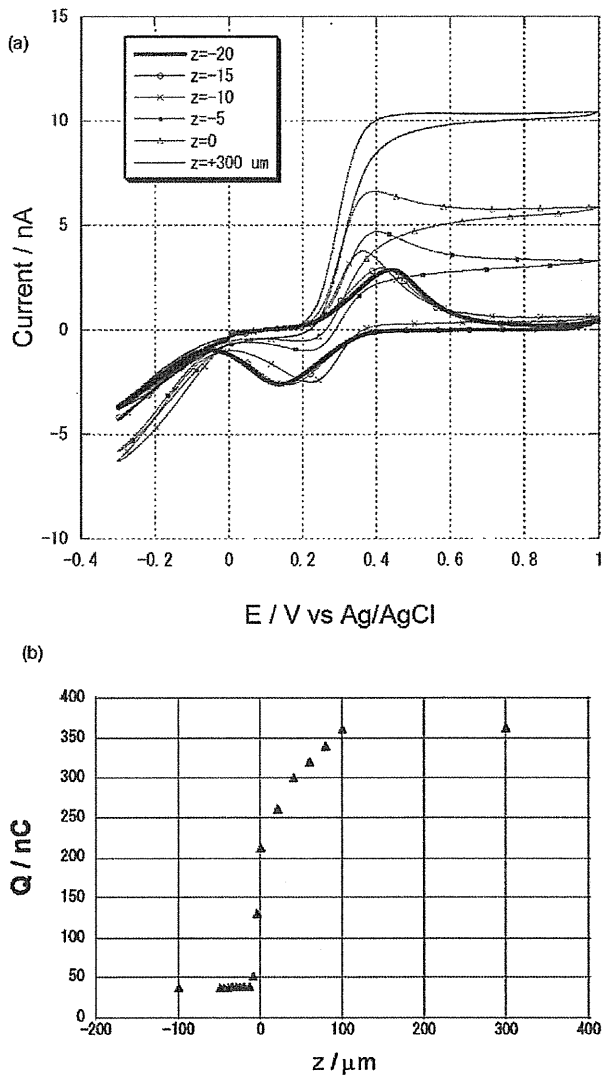

Fig. 2 (a) Cyclic voltammograms in 4 mM $K_4Fe(CN)_6$/0.1 M KCl for the PDMS microwell. Scan rate: 20 mV s^{-1}. The microelectrode was located at various *z*-positions (+300 to −20 μm). The point at $z = 0$ was defined as that where the tip touched the top of the PDMS microwell. (b) Plot of the electric charge *versus* z (+300 to −100 μm). Tip radius: 10.5 μm; Insulator radius: 85 μm.

steady state in the positive potential region. The shape of the voltammogram drastically changed at $z = 0$, showing an oxidation peak at +0.4 V due to the limited diffusion. For *z* values less than −10 μm, the oxidation current in the positive potential region (more positive than +0.7 V) was found to become almost zero, indicating that $Fe(CN)_6^{4-}$ in the microwell was almost completely consumed. When the potential was scanned in the negative direction, a reduction peak was observed at +0.15 V. The reduction current observed in less than −0.05 V originates from the oxygen dissolved in the solution.[12,42] The relatively large peak separation of 0.35 V is mainly due to the solution resistance, which depends on several parameters of the experimental setup, including the seal size of the tip electrode and the position of the tip (*z*). The electric charges estimated from the areas under the oxidation and reduction peaks were 38 and 32 nC, respectively.

Fig. 2(b) shows the plot of the electric charge of the oxidation peak as a function of *z*. The charge was almost constant (38.22 ± 0.143 nC) when the *z* value was less than −15 μm. This result suggests that the confined volume (96 pL) in the present experimental setup is preserved, regardless the position of the microelectrode tip in the relatively wide range, $z = -15$ to −100 μm. Therefore, we can precisely analyze the electrochemical behavior in the small volume of the confined cavity formed with the PDMS microwell and microelectrode cap. In this article, the electrochemical measurements for the yeast cells entrapped in the PDMS microwell were performed at $z = -30$ μm. The

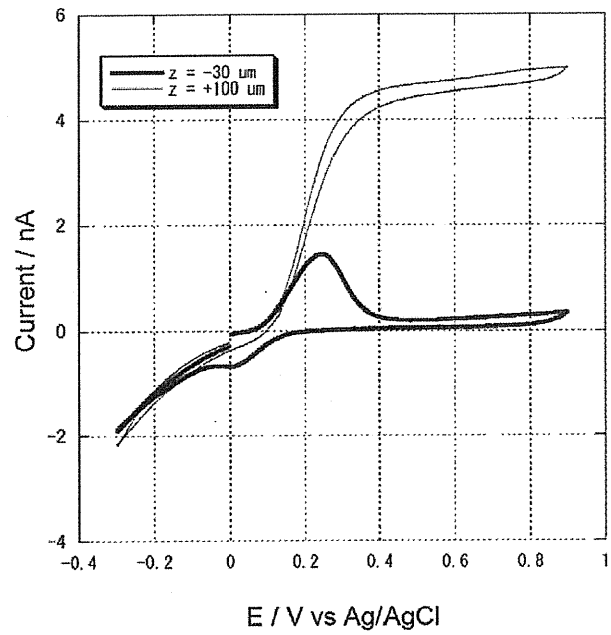

Fig. 3 Cyclic voltammograms in 0.82 mM PAP/Z-buffer for the PDMS microwell. Scan rate: 20 mV s^{-1}. The microelectrode was located attaching ($z = -30$ μm) or far from the PDMS microwell ($z = +100$ μm). Tip radius: 12 μm.

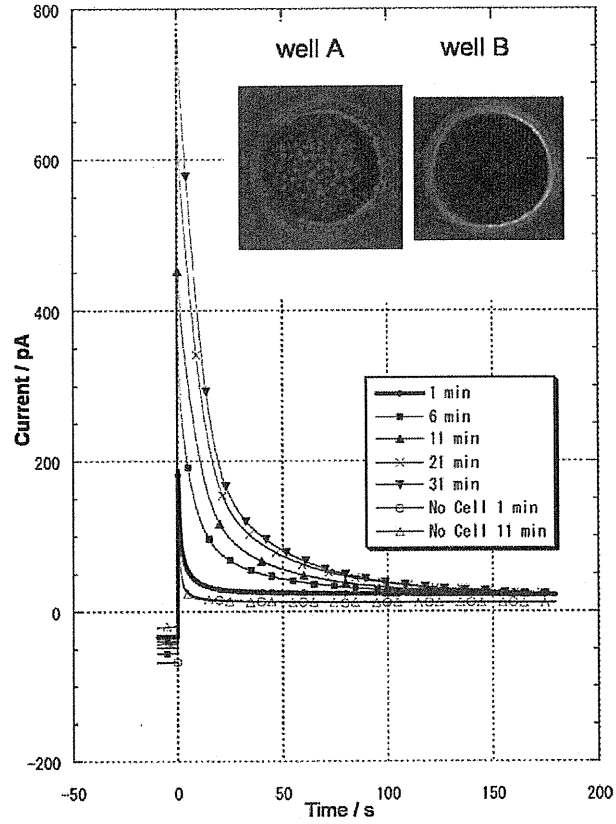

Fig. 4 Chronoamperometric results for the PDMS microwell entrapping 144 yeast cells. Before the potential was stepped from 0 V to +0.3 V, the microelectrode tip was positioned to cover the top of the PDMS microwell for various t_{accu}, from 1 to 31 min (t_{accu} = 1, 6, 11, 21, 31 min). The same procedures were also performed for the PDMS well without the yeast cells. Measuring solution: 7.4 mM PAPG, 0.3% Triton-X100T, Z-buffer. Tip radius: 12 μm. Inset: photograph of the PDMS microwells measured with (well A) and without (well B) yeast cells.

experimental setup we introduce here requires a probe positioner but need not control the vertical position with less than 10 μm preciseness. Since the microwell is made of a PDMS elastomer, the tip and microwell are less likely to damage, and therefore, both can be used repeatedly. There exist many other methods for carrying out small-volume electrochemistry using paraffin oil,[21,23] mercury,[28] oil/water droplets,[19,22] or various microfabricated 3D structures.[14–18] The present method utilizing the PDMS microwell has great advantages from the viewpoints of cost, simplicity, reproducibility, and throughput. The CV of 0.82 mM PAP oxidation within the microwell was also performed and shown in Fig. 3. At +0.3 V, the PAP oxidation current could be obtained whereas PAPG not oxidized.[29,41] The charge for the PAP oxidation 14.9 ± 0.95 nC ($n = 8$) was in good agreement with the expected theoretical value 15.3 nC in the confined microwell of 96 pL. The CV behaviours of the PAP for near ($z = -30$ μm) and far from the PDMS ($z = +100$ μm) are basically the same tendencies as those of the $K_4Fe(CN)_6$ system, however, when the potential was scanned back in the negative direction, a reduction peak was small at $z = -30$ μm probably because the product from the PAP oxidation, QI was not chemically stable.

Next, we quantitatively determined the amount of PAP produced by βGAL in the yeast cells. Fig. 4 shows the results of the chronoamperometry on the PDMS microwell entrapping 144 yeast cells. Before the potential was stepped from 0 V to +0.3 V to detect PAP, the microelectrode tip was positioned to cover the top of the PDMS microwell for different accumulation times (t_{accu} = 1–31 min), and the current responses obtained without the yeast cells (t_{accu} = 1, 11 min) were recorded. The current responses obtained with the yeast cells were considerably larger than those obtained without the yeast cells. We calculated the electric charge and time integration of the current to quantitatively evaluate the βGAL activity. The charges obtained for t_{accu} = 1 min and 11 min are approximately 5 nC and 11 nC, respectively. The 6 nC increase in the charge during the accumulation time clearly indicates that PAP is produced by the βGAL activity in the yeast cells, and is accumulated in the PDMS microwell within 10 min. When yeast cells do not exist, the background charge was independent of t_{accu}. The baseline current at 0 V fluctuated between −95 and −145 pA ($n = 12$, data not shown), probably due to the reduction in the concentrations of the dissolved oxygen and PAPG;[40] however, the background charges recorded at the +0.3 V potential step was almost constant (~3 nC). This low background charge is probably due the oxidation of PAP produced from PAPG *via* chemical (nonenzymatic) hydrolysis in solution.

Fig. 5 and 6 show the plots of the electric charge and enzymatic activity, respectively, as a function of t_{accu}. The measurements were performed three times, and the standard deviation (SD) was 2.2 to 7.8% of the each average value. The electric charge was converted to the βGAL activity (PAP product/mol s^{-1} cell $^{-1}$) by using the reaction electron number for PAP ($n_{ET} = 2$) and the Faraday constant (96500 C mol^{-1}). Fig. 5 illustrates that the

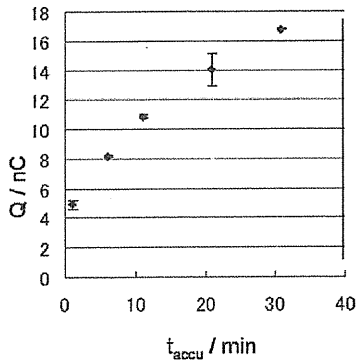

Fig. 5 Plot of the electric charge *versus* t_{accu}. The measurement was performed thrice under each set of experimental conditions ($n = 3$).

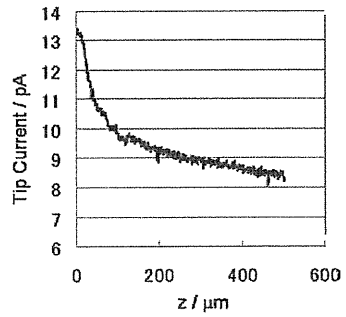

Fig. 7 Oxidation current profile as a function of the height (z) from the top of the PDMS well entrapping 86 yeast cells recorded at the center of the well in the measuring solution of 7.4 mM PAPG, 0.3% Triton-X100T, Z-buffer. Tip scan rate: 9.8 μm s^{-1}; Tip potential: +0.3 V *vs.* Ag/AgCl; Tip radius: 12 μm.

accumulation of PAP in the pL level of small volume chamber has been successfully detected. However, it should be noted that the PAP accumulation rate is not liner to t_{accu} and that the βGAL activity deceases with t_{accu} as shown in Fig. 6.

This type of confined PDMS microwell system allows another electrochemical analysis categorized in a steady-state method. In Fig. 4, the oxidation current for the microwell with 144 yeast cells is greater than that for the microwell without yeast cells by 11 pA, even 150 s after the potential step. This phenomenon implies that the rate of PAP production by yeast cells is equal to the rate of oxidation of PAP at the microelectrode, and the overall processes in the microwell reach the steady state. Under these circumstances, the βGAL activity can also be evaluated from the steady-state oxidation current; this value was found to be 3.96×10^{-19} mol s^{-1} $cell^{-1}$, which corresponded well with the value estimated from the PAP accumulation experiment shown in Fig. 6. This consistency in the values was unexpected because the steady-state method is principally different from the PAP accumulation technique, even though both can be carried out in the confined PDMS microwell system. For example at $t_{accu} = 31$ min, PAP accumulated within the microwell is estimated to be 8.8×10^{-14} mol, which corresponds to 12% of the initial amount of PAPG (7.26×10^{-13} mol) in the PDMS microwell whereas the PAP concentration is almost zero when the PAP oxidation current is in the steady state (150 s after the potential step to 0.3 V was applied).

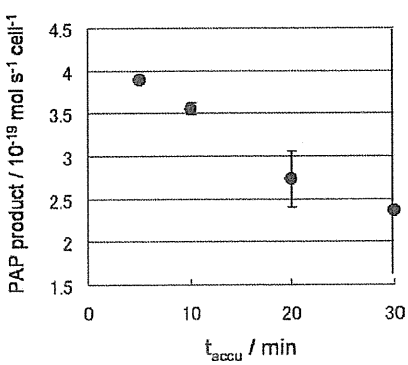

Fig. 6 Enzymatic activity (PAP production rate per cell) as a function of t_{accu}.

Finally, the βGAL activity of yeast in the PDMS microwell was evaluated by the open-system method based on the spherical diffusion theory. In this method, the concentration profile of PAP was measured keeping the microwell uncovered. When a biologically active sample is localized at a spot on a solid support, the reactant and/or product forms a spherical concentration profile near the sample.[43,44] The mass transfer rate can be obtained by employing Fick's diffusion equation. Fig. 7 shows the oxidation current profile at the central axis of the well as a function of the height (z) from the top surface of the PDMS well entrapping 86 yeast cells. The tip scan rate and tip potential were set at 9.8 μm s^{-1} and +0.3 V, respectively. The tip current was converted to the PAP concentration using a calibration curve ($[C_{PAP}/mM] = 1.558 \times 10^{-1} \times [I/nA]$ for Fig. 7). The process for estimating the mass transfer rate from the spherical concentration profile has been described elsewhere.[43] The mass transfer rate for PAP production in the open system was estimated to be 4.91×10^{-18} mol s^{-1} $cell^{-1}$ by using the diffusion coefficient of PAP, 7.1×10^{-6} cm^2 s^{-1}.[45] For comparison, the PAP accumulation experiments were also performed using the same microwell accommodating 86 yeast cells, and the PAP production rate in this case was found to be 3.73×10^{-19} mol s^{-1} $cell^{-1}$ at $t_{accu} = 11$ min, which corresponded to only 7.6% of the βGAL activity obtained in the open system. By comparing the two experimental systems for several PDMS microwells accommodating 39–144 yeast cells ($n = 6$), we found that the βGAL activity in the confined PDMS microwell system is 4.3–16.3% of that in the open system. These results claim that the cellular enzymatic and metabolic activities may be strongly affected by the microenvironmental conditions, including the size and shape of the microwell and the density of the cellular sample in the microwell. In the case of the open system, the substrate, PAPG, could be supplied very quickly. However, as the PAPG is present in excess (7.4 mM) even in the confined PDMS microwell system, the supply rate does not cause any significant difference in the PAP production activity. Quinone imine (QI), the product of the electro-oxidation of PAP, has a relatively higher chemical activity than PAPG or PAP; further, it does not diffuse in the confined PDMS microwell system. However, in the open system

shown in Fig. 7, QI produced at the scanning tip could be easily diluted. As shown in Fig. 4, the βGAL activity does not change and shows a good reproducibility when the same experiment is performed for three times, even at $t_{accu} = 31$ min; therefore, the βGAL inhibition by QI might not be irreversible.

4. Conclusions

A confined small volume was formed using a PDMS microwell array and a cap microelectrode with a relatively large seal radius. In the cyclic voltammetric measurements, the ferrocyanide ion entrapped in the microwell was oxidized with 100% efficiency, suggesting that a reproducible and quantitative electrochemical analysis was possible using this device. We also succeeded in evaluating the βGAL activity of recombinant yeast cells in the confined PDMS microwell. βGAL catalyzes the hydrolysis of PAPG to produce PAP, which is accumulated in the microwell. The accumulated PAP was quantitatively detected by amperometry using the abovementioned device. We have evaluated the βGAL activity by three different methods: the accumulation method, steady-state method, and open-system method. The βGAL activity estimated by the accumulation method was in good agreement with that estimated by the steady-state method. However, these βGAL activities estimated in the confined PDMS microwell were found to be considerably smaller than those estimated by the open-system method based on the spherical diffusion theory. This remarkable difference in the activities is probably because the concentrations of QI near the yeast cells are expected to be smaller for the open PDMS microwell than for the confined PDMS microwell. From the results obtained in the present work, we conclude that the cellular metabolic and enzymatic activities are considerably affected by the environmental conditions near the sample cells.

Acknowledgements

This work was partly supported by Grants-in-Aid for Scientific Research (18101006 and 19750055) from the Ministry of Education, Culture, Sports, Science and Technology (MEXT) and by the R & D Project for Environmental Nanotechnology from the Ministry of Environment.

References

1 C. Yi, C.-W. Li, S. Ji and M. Yang, *Anal. Chim. Acta*, 2006, **560**, 1–23.
2 C. N. LaFratta and D. R. Walt, *Chem. Rev.*, 2008, **108**, 614–637.
3 P. S. Dittrich and A. Manz, *Nat. Rev. Drug Discovery*, 2006, **5**, 210–218.
4 S. Yamamura, H. Kishi, Y. Tokimitsu, S. Kondo, R. Honda, S. R. Rao, M. Omori, E. Tamiya and A. Muraguchi, *Anal. Chem.*, 2005, **77**, 8050–8056.
5 I. Biran and D. R. Walt, *Anal. Chem.*, 2002, **74**, 3046–3054.
6 R. D. Whitaker and D. R. Walt, *Anal. Biochem.*, 2007, **360**, 63–74.
7 Y. Rondelez, G. Tresset, K. V. Tabata, H. Arata, H. Fujita, S. Takeuchi and H. Noji, *Nat. Biotechnol.*, 2005, **23**, 361–365.
8 L. Cai, N. Friedman and X. S. Xie, *Nature*, 2006, **440**, 358–362.
9 A. Groisman, C. Lobo, H. Cho, J. K. Campbell, Y. S. Dufour, A. M. Stevens and A. Levchenko, *Nat. Methods*, 2005, **2**, 685–649.
10 F. K. Balagadde, L. You, C. L. Hansen, F. H. Arnold and S. R. Quake, *Science*, 2005, **309**, 137–140.
11 W. DiLuzio, L. Turner, M. Mayer, P. Garstecki, D. B. Weibel, H. C. Berg and G. M. Whitesides, *Nature*, 2005, **435**, 1271–1274.
12 T. Saito, C.-C. Wu, H. Shiku, T. Yasukawa, M. Yokoo, T. Ito-Sasaki, H. Abe and T. Matsue, *Analyst*, 2006, **131**, 1006–1011.
13 Z. Lin, Y. Takahashi, Y. Kitagawa, T. Umemura, H. Shiku and T. Matsue, *Anal. Chem.*, 2008, **80**, 6830–6833.
14 W. Cheng, N. Klauke, H. Sedgwick, G. L. Smith and J. M. Cooper, *Lab Chip*, 2006, **6**, 1424–1431.
15 X. Cai, N. Klauke, A. Glidle, P. Cobbold, G. L. Smith and J. M. Cooper, *Anal. Chem.*, 2002, **74**, 908–914.
16 C. D. T. Bratten, P. H. Cobbold and J. M. Cooper, *Anal. Chem.*, 1998, **70**, 1164–117.
17 Z. P. Aguilar, W. R. Vandaveer and I. Fritsch, *Anal. Chem.*, 2002, **74**, 3321–3329.
18 J. C. Ball, D. L. Scott, S. Daunert, J. Wang and L. G. Bachas, *Anal. Chem.*, 2000, **72**, 497–501.
19 K. Nakatani, M. Sudo and N. Kitamura, *J. Phys. Chem. B*, 1998, **102**, 2908–2913.
20 N. Gao, X. Wang, L. Li, X. Zhang and W. Jin, *Analyst*, 2007, **132**, 1139–1146.
21 T. Yasukawa, A. Glidle, J. M. Cooper and T. Matuse, *Anal. Chem.*, 2002, **74**, 5001–5008.
22 R. Kashyap and M. Gratzl, *Anal. Chem.*, 1998, **70**, 1468–1476.
23 R. A. Clark, P. B. Hietpas and A. G. Ewing, *Anal. Chem.*, 1997, **69**, 259–263.
24 G. Wittstock, M. Burchardt, S. E. Pust, Y. Shen and C. Zhao, *Angew. Chem., Int. Ed.*, 2007, **46**, 1584–1617.
25 A. Schulte and W. Schuhmann, *Angew. Chem., Int. Ed.*, 2007, **46**, 8760–8777.
26 P. Sun and M. V. Mirkin, *Anal. Chem.*, 2007, **79**, 5809–5816.
27 F.-R. F. Fan, J. Kwak and A. J. Bard, *J. Am. Chem. Soc.*, 1996, **118**, 9669–9675.
28 M. V. Mirkin, L. O. Bulhoes and A. J. Bard, *J. Am. Chem. Soc.*, 1993, **115**, 201–204.
29 T. Yasukawa, K. Nagamine, Y. Horiguchi, H. Shiku, M. Koide, T. Itayama, F. Shiraishi and T. Matsue, *Anal. Chem.*, 2008, **80**, 3722–3727.
30 M. Badihi-Mossberg, V. Buchner and J. Rishpon, *Electroanalysis*, 2007, **19**, 2015–2028.
31 A. Schwartz-Mittelman, A. Baruch, T. Neufeld, V. Buchner and J. Rishpon, *Bioelectrochemistry*, 2005, **65**, 149–156.
32 A. Schwartz-Mittelman, T. Neufeld, D. Biran and J. Rishpon, *Anal. Biochem.*, 2003, **317**, 34–39.
33 J. Nishikawa, K. Saito, J. Goto, F. Dakeyama, M. Matsueo and T. Nishihara, *Toxcol. Appl. Pharmacol.*, 1999, **154**, 76–83.
34 F. Shiraishi, H. Shiraishi, J. Nishikawa, T. Nishihara and M. Morita, *J. Environ. Chem.*, 2000, **10**, 57–64.
35 S. Arulmozhiraja, F. Shiraishi, T. Okumura, M. Iida, H. Takigami, J. S. Edmonds and M. Morite, *Toxicol. Sci.*, 2005, **84**, 49–62.
36 C. K. Chow and S. P. Palecek, *Biotechnol. Prog.*, 2004, **20**, 449–456.
37 I. Biran, L. Kilmenty, R. H. Aronis, E. Z. Ron and J. Rishpon, *Microbiology*, 1999, **145**, 2129–2133.
38 T. Kaya, K. Nagamine, N. Matsui, T. Yasukawa, H. Shiku and T. Matsue, *Chem. Commun.*, 2004, 248–249.
39 K. Nagamine, S. Onodera, A. Kurihara, T. Yasukawa, H. Shiku, R. Asano, I. Kumagai and T. Matsue, *Biotechnol. Bioeng.*, 2007, **96**, 1008–1013.
40 C. Zhao, J. K. Sinha, C. A. Wijayawardhana and G. Wittstock, *J. Electroanal. Chem.*, 2004, **561**, 83–91.
41 N. Matsui, T. Kaya, K. Nagamine, T. Yasukawa, H. Shiku and T. Matsue, *Biosens. Bioelectron.*, 2006, **21**, 1202–1209.
42 H. Shiku, T. Saito, C.-C. Wu, T. Yasukawa, M. Yokoo, H. Abe, T. Matsue and H. Yamada, *Chem. Lett.*, 2006, **35**, 234–235.
43 T. Kaya, D. Numai, K. Nagamine, S. Aoyagi, H. Shiku and T. Matsue, *Analyst*, 2004, **129**, 529–534.
44 H. Shiku, T. Shiraishi, S. Aoyagi, Y. Utsumi, M. Matsudaira, H. Abe, H. Hoshi, S. Kasai, H. Ohya and T. Matsue, *Anal. Chim. Acta*, 2004, **522**, 51–58.
45 O. Niwa, Y. Xu, H. B. Halsall and W. R. Heineman, *Anal. Chem.*, 1993, **65**, 1559–1563.

Analytica Chimica Acta 640 (2009) 87–92

Contents lists available at ScienceDirect

Analytica Chimica Acta

journal homepage: www.elsevier.com/locate/aca

Development of electrochemical reporter assay using HeLa cells transfected with vector plasmids encoding various responsive elements

Hitoshi Shiku[a,*], Michiaki Takeda[a], Tatsuya Murata[a], Uichi Akiba[b], Fumio Hamada[b], Tomokazu Matsue[a,**]

[a] Graduate School of Environmental Studies, Tohoku University, 6-6-11-604 Aramaki-Aoba, Sendai 980-8579, Japan
[b] Graduate School of Engineering & Resource Science, Akita University, 1-1 Tegata gakuen-machi, Akita 010-8502, Japan

ARTICLE INFO

Article history:
Received 27 December 2008
Received in revised form 11 March 2009
Accepted 12 March 2009
Available online 20 March 2009

Keywords:
Reporter assay
Scanning electrochemical microscopy
Chemiluminescence
Responsive element
Signal transduction
Alkaline phosphatase

ABSTRACT

Electrochemical assay using HeLa cell lines transfected with various plasmid vectors encoding SEAP (secreted alkaline phosphatase) as the reporter has been performed by using SECM (scanning electrochemical microscopy). The plasmid vector contains different responsive elements that include GRE (glucocorticoid response elements), CRE (cAMP responsive elements), or κB (binding site for NFκB (nuclear factor kappa B)) upstream of the SEAP sequence. The transfected HeLa cells were patterned on a culture dish in a 4 × 4 array of circles of diameter 300 μm by using the PDMS (poly(dimethylsiloxane)) stencil technique. The cellular array was first exposed to 100 ng mL^{-1} dexamethasone, 10 ng mL^{-1} forskolin, or 100 ng mL^{-1} TNF-α (tumor necrosis factor α) after which it was further cultured in an RPMI culture medium for 6 h. After incubation, the cellular array was soaked in a measuring solution containing 4.7 mM PAPP (p-aminophenylphosphate) at pH 9.5, following which electrochemical measurements were performed immediately within 40 min. The SECM method allows parallel evaluation of different cell lines transfected with pGRE-SEAP, pCRE-SEAP, and pNFκB-SEAP patterned on the same solid support for detection of the oxidation current of PAP (p-aminophenol) flux produced from only 300 HeLa cells in each stencil pattern. The results of the SECM method were highly sensitive as compared to those obtained from the conventional CL (chemiluminescence) protocol with at least 5 × 10^4 cells per well.

1. Introduction

Whole-cell biosensors refer to electrochemical and/or optical biosensors that utilizes "whole cells" instead of purified enzymes for converting specific chemical inputs into signals. Gene engineering has been evolutionally expanded the field of the cell-based biosensor because the genetically modified cell itself functions as a transducer to produce a measurable signal, reporter protein such as green fluorescence protein, chloramphenicol acetyl transferase, luciferase, beta-galactosidase, or secreted alkaline phosphatase (SEAP). These proteins are generated in response to various analytes that possibly activate/suppress gene expressions at a transcriptional level [1,2]. The reporter assay is frequently used by introducing a vector plasmid containing the sensing element upstream of a reporter gene. Sensitive and selective detection of metals, hydrocarbons, mutagens, and pollutants can be achieved by the use of genetically engineered whole-cell biosensors [1]. More importantly, the whole-cell reporter assay allows the evaluation of signal pathways that are activated, namely the intracellular mechanisms of action against specific drugs and toxins [3–5]. Expression vectors, which contain reporter genes controlled by a specific transcription factor consensus sequence, are used to study transcription factors and cellular signaling mechanisms. In fact, there are several commercially available kits that can determine the involvement of various response element-binding proteins in signal transduction pathways. Parallel evaluation of signaling pathways can be accomplished by combining cellular array technology with cells transfected with different types of plasmid vectors [6].

Recent advances in microfluidics and sensor miniaturization have resulted in rapid, cheap, and integrated analysis using closed microfluidic systems [7–9]. Cellular array chips play a significant role in realizing a high-throughput screening, especially in a manner similar to reverse transfection [10–12]. Gene introduction on cellular chips is not always helpful because of increase in the heterogeneity of the cellular status, low reliability, and a long assay time. We have developed various types of cellular chips on which cell culture [13–16], differentiation [17–19], manipulation [20–22], stimulation [23], gene introduction [24], and controlling of cellular polarity processes [25] were electrochemically detected. In many cases chemical stimulation of cells for gene expression was carried

* Corresponding author. Tel.: +81 22 795 6167; fax: +81 22 795 6167.
** Corresponding author.
E-mail addresses: shiku@bioinfo.che.tohoku.ac.jp (H. Shiku), matsue@bioinfo.che.tohoku.ac.jp (T. Matsue).

0003-2670/$ – see front matter © 2009 Elsevier B.V. All rights reserved.
doi:10.1016/j.aca.2009.03.018

out in the pre-culture stage before immobilizing the cells on the chip, since it could not be accomplished on a chip [17,18,21,22,26].

In the present study, cells transfected with different plasmid constructs were cultured as monolayers on a stencil-masked solid support [27–30]. Cellular signal transduction is triggered with the help of chemical stimulation performed on a solid support. To obtain parallel responses from each of the cell lines with a certain number of cells (300 cells arranged in a circular pattern with a diameter of 300 μm), the stencil sheet was peeled off just before the electrochemical measurement to form the cellular pattern. The expression of SEAP was electrochemically evaluated after stimulating each signal transduction pathway with the triggering chemicals. The cellular status in the monolayer culture system used in the present study was also evaluated for the stencil-based culture in the medium after exchanging it with the measuring solution (pH 9.5).

2. Experimental

2.1. Materials

p-Aminophenol (PAP, Wako Pure Chemical Industries), dexamethasone (Wako Pure Chemical Industries), forskolin (Sigma), tumor necrosis factor α (TNF-α, Wako Pure Chemical Industries), 2-[4-(2-hydroxyethyl)-1-piperazinyl] ethanesulfonic acid (HEPES, Dojindo Laboratories, Japan), 3,3,4,4,5,5,6,6,6,-nonafluorohexyltrichlorosilane (LS-912, Shin-etsu Chemical Co. Ltd.), RPMI-1640 (Gibco Invitrogen, Tokyo, Japan), fetal bovine serum (FBS, Gibco), collagen type I-A (Nitta Gelatin, Japan), penicillin (Gibco), streptomycin (Gibco), Mercury™ pathway profiling system (BD Sciences), Opti-MEM I medium (Gibco), LipofectAMINE 2000 (Invitrogen), poly(dimethylsiloxane) (PDMS, Silpot 184W/C, Dow Corning, USA), and others chemicals were used as received. The Mercury™ pathway profiling system is a set of expression vector sets that contain a distinct enhancer element upstream of a reporter gene—SEAP. Various intracellular signal transduction pathways were assessed by employing these vector sets with their corresponding enhancer elements—GRE (glucocorticoid response elements), CRE (cAMP response element), κB (kappa B), AP1 (activator protein 1), HSE (heat shock element), NFAT (nuclear factor of activated T cells), Myc (E-box DNA binding protein), and SRE (serum-response element). Three of the eight reporter genes showed activity above baseline after a 24-h stimulation—GRE, CRE, and NFκB. The responsive elements GRE, CRE, and κB are specific DNA sequences called enhancers to which the transcription factors GREB (GRE binding protein), CREB (CRE binding protein), and NFκB (nuclear factor κB) bind. The pSEAP2 series is an integrated set of plasmids that differs only with regard to the presence or absence of the simian virus 40 (SV40) promoter and/or enhancer sequence. The pSEAP2-Control vector contains the SEAP structural gene that is under the transcriptional control of the SV40 promoter and enhancer, whereas the pSEAP2-basic vector contains the SEAP gene without promoter/enhancer. p-Aminophenylphosphate (PAPP) monosodium salt was purchased from LKT Lab Inc. or synthesized according to the procedure described in the literature [31,32].

2.2. Cell culture and transfection

HeLa cells were donated by the Cell Resource Center for Biomedical Research (Tohoku University). The cells were cultured in RPMI-1640 containing 10% FBS, 50 μg mL^{-1} penicillin, and 50 μg mL^{-1} streptomycin at 37 °C in a humidified atmosphere containing 5% CO_2. HeLa cells were transfected with the expression vector set of Mercury™ Pathway Profiling System. The cells were seeded in a 35-mm dish (Falcon) at a density of 5×10^5 cells in 2 mL of RPMI-1640 medium containing 10% FBS without antibiotics. A day after the cultivation, transfection was performed by the addition of 500 μL of Opti-MEM I medium containing 4 μg of plasmid DNA and 10 μL of LipofectAMINE 2000; then, incubation was carried out for 5 h. Subsequently, the transfection medium changed to a pure culture medium, and the cells were incubated at 37 °C overnight.

2.3. Electrochemical assay of cellular array patterned using a PDMS stencil technique

The transfected HeLa cells were patterned on a culture dish in an array of circles of diameter 300 μm by using a PDMS stencil. A PDMS stencil sheet of a thickness of 100 μm was prepared from a PDMS-curing agent mixture (10:1, w/w), and the thickness of the PDMS sheet was controlled by a spin coater (1000 rpm, 30 s). The fabrication procedure is described elsewhere [33,34]. In the PDMS stencil, the 4 × 4 hole-array of diameter 300 μm was drawn using a CO_2 laser engraving system (Universal Laser System Inc.) and treated with an O_2 plasma (plasma asher LTA-101, Yanaco, 100 W, 13.6 MHz, 15 s, O_2 flow rate: 40 mL min^{-1}). The PDMS stencil sheet was soaked into a 70% ethanol solution for 30 min and placed at the bottom of the culture dish of diameter 35 mm; the sheet was then placed on a clean bench and irradiated with a UV lamp for 30 min. The HeLa cells were suspended in a medium to achieve a final concentration of 1.5×10^6 cells mL^{-1}; 150 μL of this suspension was seeded into the PDMS stencil. The stencil was then incubated for 4 h at 37 °C in a humidified atmosphere containing 5% CO_2. Two milliliters of the medium, which included the stimulation chemical reagent (final concentrations: 100 ng mL^{-1} dexamethasone, 10 μg mL^{-1} forskolin, or 100 ng mL^{-1} TNF-α), was added and further incubated for 6–24 h at 37 °C in a humidified atmosphere containing 5% CO_2. Stock solutions of dexamethasone and forskolin were diluted with dimethyl sulfoxide (DMSO, Wako Pure Chemical Industries) and stored at −20 °C. Dexamethasone, forskolin, and TNF-α were selected as the characteristic stimuli for the signaling pathways of GRE, PKC (protein kinase C)/CREB, and NFκB, respectively.

The scanning electrochemical microscope consisted of a Pt microdisk (diameter: 20 μm) as the working electrode and a Ag/AgCl reference/counter electrode [3,35]. The electrode potential was set at 0.3 V vs Ag/AgCl for facilitating the oxidation of PAP. For the SECM measurements, the PDMS stencil sheet was peeled off and the culture dish was immediately washed twice with HEPES buffer and was placed into 2 mL of the measuring solution containing 4.7 mM PAPP and HEPES buffer (pH 9.5). The electrochemical measurements were completed within 5 min for each line scan of 1500 μm at a rate of 50 μm s^{-1} at room temperature. Normally, SECM imaging with a resolution of 1000 μm × 1000 μm takes approximately 30 min (20 lines at 20 μm s^{-1}). The tip-scanning height from the substrate surface was set at 50 μm. Viability of the cells patterned on the stencil, under the conditions used during SECM measurements was evaluated by a live/dead fluorescence kit (a combination of two fluorochromes, calcein-AM and propidium iodide, Dojindo Laboratories, Japan). The results of the evaluation indicated that almost all the cells were alive for a period of 60 min after they were soaked in the measuring solution (pH 9.5). For static analysis, the SECM measurement was repeated for more than six times ($n \geq 6$) in order to compare the current responses with and without stimulation for each of the transfected HeLa cell lines.

2.4. Chemiluminescence (CL) SEAP assay

The SEAP activity was evaluated using a Great EscAPe™ SEAP chemiluminescence detection kit (BD Sciences) in accordance with the recommended protocol [3]. Briefly, the transfected HeLa cells were seeded in collagen-coated 96-well plates (Cellmatrix Type I-C, Nitta Gelatin) at a rate of 5×10^5 cells per well and were incubated for 4 h. After observation of cell adhesion, a stimulus solution was added, and the cells were further incubated for 24 h. Fifteen microliters of the culture medium was sampled from each well for the CL SEAP assay. The sampled culture medium was mixed with 45 μL of dilution buffer and incubated at 65 °C for 30 min in order to inhibit endogenous phosphatase activity. Since the reporter proteins SEAP and SEAP2 were heat protective, only the expressing SEAP activity could be measured after the heat shock. The sample was first mixed with 60 μL of the assay buffer (pH 10.3) for 5 min at room temperature and then with 60 μL of the chemiluminescence solution containing 1.25 mM CSPD (disodium 3-(4-methoxyspiro [1,2-dioxetane-3,2′-(5′-chloro)-tricyclo [3,3,1,1^{3,7}]decan]-4-yl)phenyl phosphate). After incubating the sample in the dark for 10 min, the CL signals were detected using a high-performance intensified CCD camera (PI-MAX 512RB, Princeton Instruments) [3,19]. The assays were repeated thrice under each experimental condition ($n = 3$).

3. Results and discussion

Fig. 1a shows the CL intensities of 5×10^4 cells of non-transfected HeLa (wild type) cells and HeLa cells transfected with the SEAP plasmids of negative (pSEAP2-Basic) and positive controls (pSEAP2-Control) according to the conventional 96-well based assay. In the CL assay protocol, 15 μL of the culture medium was required for sampling, and the sample was further treated at 65 °C for 30 min in order to deactivate the background activities of alkaline phosphatase. Fig. 1b shows the CL results obtained for the HeLa cells transfected with pGRE-SEAP, pCRE-SEAP, or pNFκB-SEAP 24 h after stimulation. Dexamethasone [6,36,37], forskolin [38], or TNF-α [6,39] was chosen as the stimulus and was compared with the cases without stimulation. As a negative control, the alkaline phosphatase activities of the HeLa cells transfected with pSEAP-Basic were also evaluated under each stimulation condition. The CL responses to stimulus exposure were precisely observed for all the transfected HeLa cell lines. The evaluated concentration ranges for the stimuli were 10–10^4 ng mL^{-1} for dexamethasone, 10–10^3 μg mL^{-1} for forskolin, and 10–100 ng mL^{-1} for TNF-α. The linearity of the calibration plot between the CL response and the stimulus concentration was poor. It was also difficult to increase the linearity of the response by increasing the concentration of the stimulus in the electrochemical assay. The values of the signal to noise ratio (S/N), which is defined as the intensity for adding stimulus normal

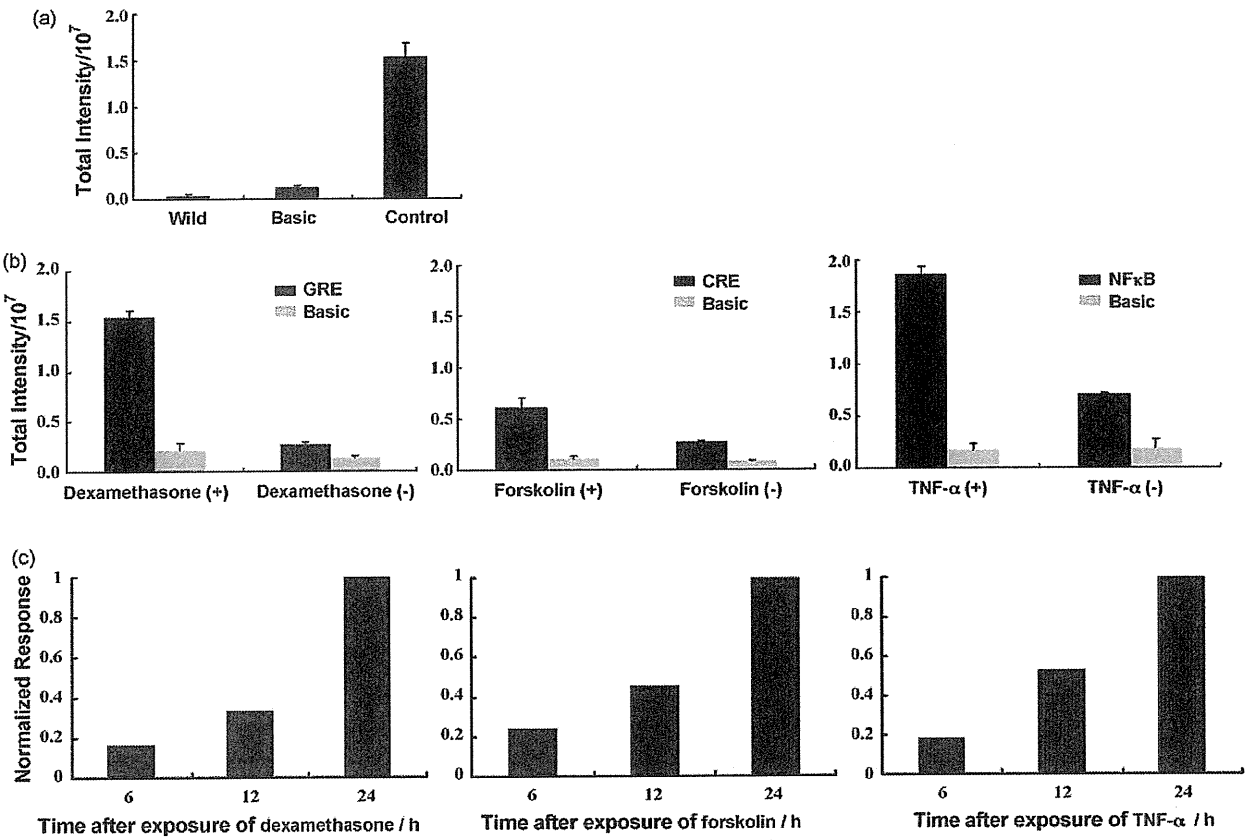

Fig. 1. (a) SEAP activity based on the CL assay for the wild-type HeLa cells and HeLa cells transfected with pSEAP2-Basic (negative control) and pSEAP2-Control (positive control). (b) CL SEAP assay for HeLa cells transfected with pGRE-SEAP, pCRE-SEAP, and pNFκB-SEAP. Dexamethasone (100 ng mL^{-1}), forskolin (10 μg mL^{-1}), and TNF-α (100 ng mL^{-1}) were added as stimuli and the results obtained were compared with those without the stimulus. (c) CL SEAP assay as a function of time after the addition of the stimulus (dexamethasone, forskolin, or TNF-α). Control indicates HeLa cells transfected with pSEAP2-Control (positive control) without the stimuli.

to that without stimulation, were 5.8, 2.2, and 2.6 for dexamethasone, forskolin, and TNF-α, respectively. In the case of the NFκB pathway stimulated with TNF-α, the signal (result obtained with stimulation) as well as the noise level (result obtained without stimulation) was the highest among the three experiments. Fig. 1c shows the CL intensities as a function of time after stimulation for HeLa cells transfected with pGRE-SEAP, pCRE-SEAP, and pNFκB-SEAP. Dexamethasone (100 ng mL^{-1}), forskolin (10 μg mL^{-1}), and

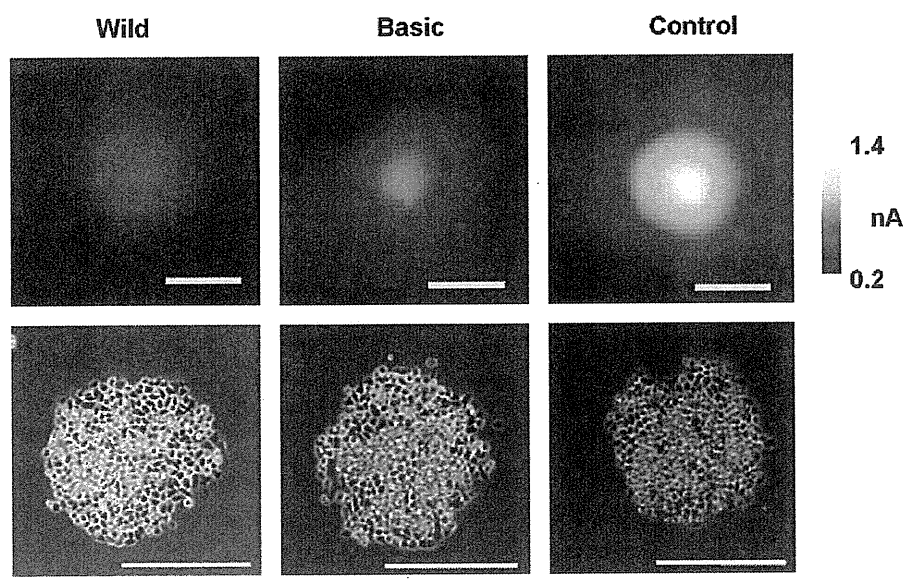

Fig. 2. SECM images of the stencil-patterned HeLa cells (~300 cells) transfected with pSEAP2-Control (positive control), pSEAP2-Basic (negative control), and the wild-type HeLa cells. A Pt disk with a diameter of 20 μm was used as the probe electrode. Optical micrographs for the corresponding HeLa cells are also shown. Bar: 300 μm.

TNF-α (100 ng mL^{-1}) were added as stimuli in the microtiter plate and incubated for 6, 12, and 24 h, respectively. HeLa cells (pSEAP2-Control) were suspended in the culture medium and incubated and used as the positive control. Since the secreted alkaline phosphatase accumulated in the medium in the microtiter plate well, the chemical intensities of all the four transfected HeLa cell lines increased linearly with the exposure time.

Fig. 2 shows the SECM images along with the corresponding optical microscope images for non-transfected HeLa cells (wild type) and HeLa cells transfected with SEAP plasmids of negative (pSEAP2-Basic) and positive controls (pSEAP2-Control) that were patterned using a PDMS stencil of diameter 300 μm. The number of cells in the patterns, which was counted manually, was found to be about 300. SEAP was secreted from the patterned cells into the surrounding medium and then the enzymatic substrate PAPP was hydrolyzed to PAP, which was electrochemically oxidized at the probe electrode. The oxidation current of 1.35 ± 0.417 nA (n = 7) for HeLa transfected with pSEAP2-Control was obtained with the substrate generation/tip collection mode SECM. It was found from a calibration curve that the oxidation current value corresponds to a local PAP concentration of ~0.45 mM, which is considerably smaller than the bulk PAPP concentration (4.7 mM). The oxidation current profiles were almost stable during the time-scale of SECM imaging (about 30 min per image) that suggested the concentration profile of PAP near the circle cellular pattern were in steady state. The PAP concentration profile was in accordance with a hemispherical diffusion theory and not disturbed by the diffusion of SEAP enzyme. Background currents for the wild-type HeLa cells and HeLa cells transfected with pSEAP2-Basic were 0.622 ± 0.042 (n = 4) and 0.731 ± 0.208 nA (n = 3), respectively. Since the levels of background currents for the two cell lines were almost similar, it could be concluded that these currents were due to the original (endogeneous) activity of alkaline phosphatase present in the HeLa cells and not due to SEAP secreted from pSEAP2-Basic.

The SECM assay is advantageous to detect the localized flux for the product (PAP) of the enzymatic reaction [26] with a probe microelectrode and a relatively small number of cells (~300) is enough to monitor the PAP concentration profile near the cellular sample. The volume of the measuring solution (2 mL) must be sufficiently large compared to the local enzymatic reaction rate, otherwise the concentration of both SEAP and PAP in bulk solution would elevate and the oxidation current profile becomes broader. On the contrary, the CL assay was performed with conventional 96-well plates. The SEAP activity within the solution of the total 180 μL was detected with a high-performance intensified CCD camera. At least 10^4 cells were required to detect CL signal in our system.

Table 1
SECM response [(average ± standard deviation)/nA] (n = sample number) for various stimulus reagents corresponding to the plasmids transfected into the HeLa cells.

	Stimulus		
	Dexamethasone	Forskolin	TNF-α
Plasmid	pGRE	pCRE	pNFκB
(+)	1.09 ± 0.175 (8)	1.46 ± 0.192 (17)	1.38 ± 0.312 (6)
(−)	0.632 ± 0.120 (8)	1.18 ± 0.102 (14)	0.861 ± 0.139 (7)
p	<0.005	<0.001	<0.005
S/N	1.73	1.23	1.60

The selection of the cell type is important to obtain sufficient reporter signals. HepG2 (human hapatoma cell line) [6], HEK293 (human embryonic kidney) [10], MCF-7 (human breast cancer cell line) [3], and HeLa cell lines were transfected with pSEAP2-Control vector and it was found that HeLa cells showed the highest gene expression activity. In the case that a MCF-7 was selected and transfected with pSEAP2-Control, the PAP oxidation current for the stencil-patterned cells was 2.0 pA with an SECM assay (data not shown). The CL evaluations demonstrated that the SEAP activity of the transfected HeLa cells was at least 4-fold larger than that of the transfected MCF-7. However, the background response for HeLa cells transfected with pSEAP2-Basic increased considerably, whereas that for MCF-7 cells transfected with pSEAP2-Basic was almost negligible.

Next the one-line SECM scans for the HeLa cells transfected with pGRE-SEAP, pCRE-SEAP, and pNFκB-SEAP were evaluated

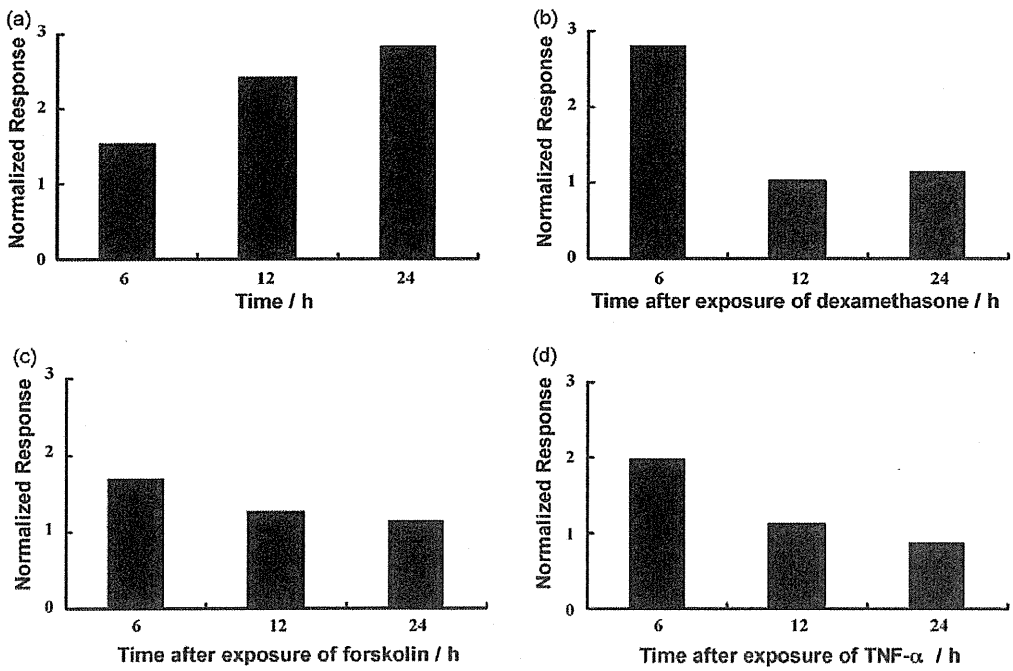

Fig. 3. SECM assay as a function of time after the addition of the stimulus (dexamethasone (b), forskolin (c), or TNF-α (d)) for the stencil-patterned HeLa cells transfected with pGRE-SEAP (b), pCRE-SEAP (c), and pNFκB-SEAP (d), respectively. Control indicates the HeLa transfected with pSEAP2-Control (positive control) without stimulus reagent (a).

with (+) and without (−) dexamethazone (100 ng mL^{-1}), forskolin (10 μg mL^{-1}), and TNF-α (100 ng mL^{-1}), respectively. Table 1 shows the summarized SECM responses for various stimulations. The response obtained 6 h after the stimulation was compared with that without the stimulation. The current response in the SECM assay is determined by subtracting the background response (the current at a distance of 600 μm from the center of the circular pattern of the HeLa cells) from current at the center. The maximum response was observed for CRE (1.46 ± 0.192 nA (n = 17)), the minimum for GRE (1.09 ± 0.175 nA (n = 8)), and an intermediate response for NFκB (1.38 ± 0.312 nA (n = 6)). The response was normalized to the corresponding result without stimulation and defined as signal to noise ratio (S/N) because the SECM response tended to vary with the cellular status of the cultured host and the transfection conditions. Typically, the current response without stimulation ranged from 0.12 to 0.6 nA, during the experiments have been performed for 1 year. The responses obtained were in the following order: GRE (S/N = 1.73) > NFκB (S/N = 1.60) > CRE (S/N = 1.23). Since the S/N ratios obtained were different from one another, all the three responses with and without the stimuli were found to be statistically distinguishable (t-test, $p < 0.005$).

Fig. 3 shows time dependency after stimulation. The SECM responses were normalized to those without stimulation. HeLa cells transfected with pSEAP2-Control were also evaluated in the medium under conditions identical to those used in the SECM measurements and normalized to the response for the HeLa transfected with pSEAP2-Basic (Fig. 3a). Among the responses (Fig. 3b–d) obtained for the three signal pathways evaluated 6 h, 12 h, and 24 h after the stimulation, the response 6 h after the stimulation was the maximum. This type of signal degradation during longer timescale incubation has also been observed in the other reporter assay systems, especially those based on electrochemical cellular chips utilizing bacteria and mammalian cells [3,17]. On the contrary, the current responses for the positive control 12 h and 24 h after incubation were almost identical to or slightly larger than those 6 h after the incubation. This result suggests that the cells patterned using the stencil technique facilitates the maintenance of cellular functions during a 24-h incubation.

Arraying cell lines transfected with different plasmids on a solid support may be the most suitable electrochemical reporter assay for the evaluation of various signaling pathways. Fig. 4a shows the responses to the one-line SECM scans for HeLa cells transfected with pGRE-SEAP, pCRE-SEAP, and pNFκB-SEAP patterned on the same culture dish 6 h after the addition of 100 ng mL^{-1} dexamethasone. The results obtained in the CL assay are also shown in Fig. 4b. Dexamethasone is known as a typical stimulus of GR pathway [36,37], and therefore, the current response is the highest for the cells transfected with pGRE-SEAP. Interestingly, the current signal for pCRE-SEAP is also significantly greater than that observed before the addition of dexamethasone. However, the signal for pNFκB-SEAP was not influenced by dexamethasone addition. The current responses obtained on a single solid support corresponded well with the CL results obtained at a level of ~10^4 cells. The responses to the one-line SECM scans for the cellular arrays of the three transfected HeLa cell lines 6 h after the addition of 10 μg mL^{-1} forskolin and 100 ng mL^{-1} TNF-α are shown in Fig. 4c and e, respectively. The

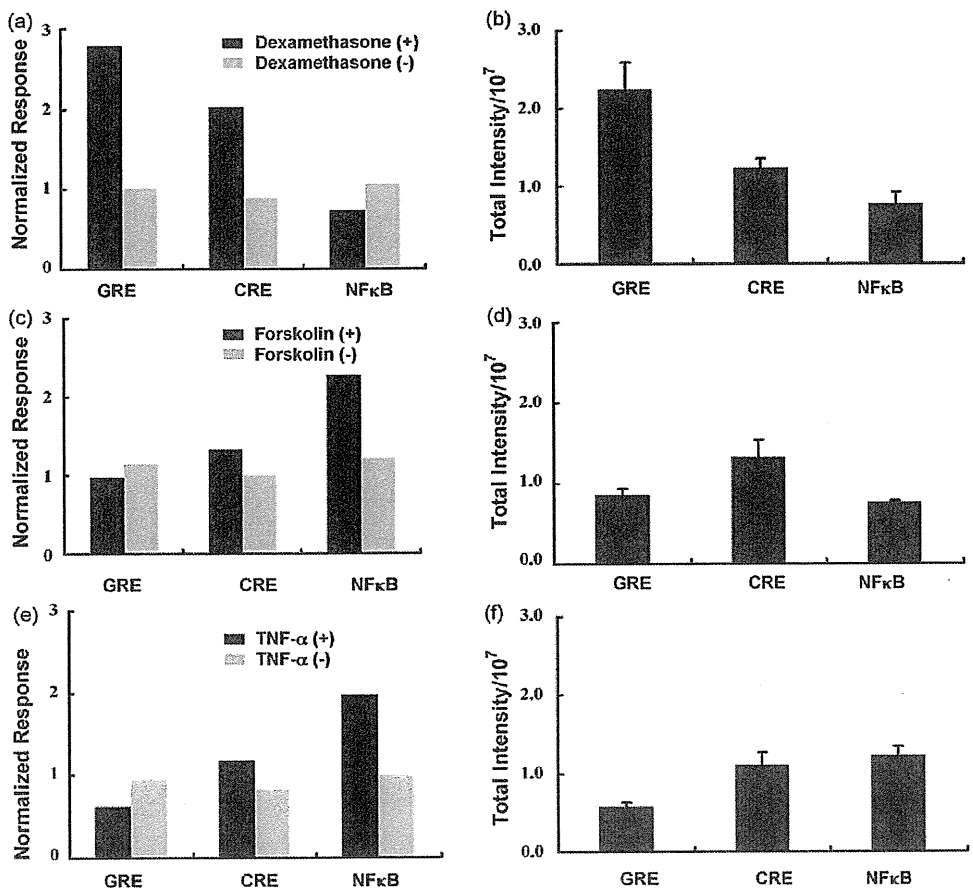

Fig. 4. SECM responses (a, c and e) of the stencil-patterned HeLa cells transfected with pGRE-SEAP, pCRE-SEAP, and pNFκB-SEAP. The results of the CL SEAP assay (b, d and f) are also shown. Dexamethasone (a and b, 100 ng mL^{-1}), forskolin (c and d, 10 μg mL^{-1}), and TNF-α (e and f, 100 ng mL^{-1}) were added as stimuli and incubated for 6 h for SECM and 24 h for CL.

results of the CL assays are shown in Fig. 4d and f. In all the cases, the electrochemical and CL results were in good agreement.

Overall, the electrochemical reporter assay may be suitable for qualitative screening but not very useful for quantitative evaluation of the calibration curves between the response and the ligand concentrations. Consequently, static analysis should be performed for each of the stimulation reagents in order to judge whether cellular signal transduction is activated or not. In the future, we plan to design an integrated electrochemical cellular device that allows a rapid and high-throughput analysis. However, as discussed in this study, SECM characterization before integration of the electrode array and the cellular chip is powerful and essential for the evaluation of certain cellular signal transduction pathways and cellular status patterned on the solid supports.

4. Conclusion

SECM was used for the preparation of an electrochemical reporter assay from HeLa cells transfected with plasmids coding various responsive elements. Genetically engineered HeLa cells were arrayed on a glass substrate with a PDMS stencil, and the cellular status of the stencil-patterned cell array was found to be normal for a 24-h incubation in a medium with various stimulus reagents as well as a 60-min exposure to the measuring solution of pH 9.5. The GRE, CRE, and NFκB signal pathways were all electrochemically monitored using the stencil-patterned HeLa cell arrays. The electrochemical responses were also compared with the results of the CL assay, which required a concentration of 5×10^4 cells per well. In contrast, the SECM assay can be performed with ~300 cells, and it neither requires medium sampling nor deactivation for inhibition of the endogenous phosphatase activity.

Acknowledgements

This work was partly supported by a Grant-in-Aid for Scientific Research on Priority Areas (17066002) "Life Surveyor" from the Ministry of Education, Culture, Sports, Science and Technology (MEXT) of Japan; by Grants-in-Aid for Scientific Research (18101006 and 19750055) from MEXT; and by a grant from the Center for Interdisciplinary Research, Tohoku University.

References

[1] S. Daunert, G. Barrett, J.S. Feliciano, R.S. Shetty, S. Shrestha, W.S. Spencer, Chem. Rev. 100 (2000) 2705–2738.
[2] T. Matsue, H. Shiku, Electrochemistry 74 (2006) 107–113.
[3] Y.S. Torisawa, N. Ohara, K. Nagamine, S. Kasai, T. Yasukawa, H. Shiku, T. Matsue, Anal. Chem. 78 (2006) 7625–7631.
[4] K.Y. Inoue, T. Yasukawa, H. Shiku, T. Matsue, Electrochemistry 76 (2008) 525–528.
[5] E. Kelso, J. McLean, M.F. Cardosi, Electroanalysis 12 (2000) 490–494.
[6] K.R. King, S. Wang, D. Irima, A. Jayaraman, M. Toner, M.L. Yarmush, Lab Chip 7 (2007) 77–85.
[7] C. Yi, C.-W. Li, S. Ji, M. Yang, Anal. Chim. Acta 560 (2006) 1–23.
[8] C.E. Sims, N.L. Allbritton, Lab Chip 7 (2007) 423–440.
[9] J. El-Ali,.P.K. Sorger, K.F. Jensen, Nature 442 (2006) 403–411.
[10] J. Ziauddin, D.M. Sabatini, Nature 411 (2001) 107–110.
[11] J.B. Delehanty, K.M. Shaffer, B. Lin, Biosens. Bioelectron. 20 (2004) 773–779.
[12] S. Fujita, E. Ota, C. Sakaki, K. Takano, M. Miyake, J. Miyake, J. Biotechnol. 104 (2007) 329–333.
[13] T. Kaya, K. Nagamine, D. Oyamatsu, H. Shiku, M. Nishizawa, T. Matsue, Lab Chip 3 (2003) 320–324.
[14] Y.S. Torisawa, T. Kaya, T. Takii, D. Oyamatsu, M. Nishizawa, T. Matsue, Anal. Chem. 73 (2003) 2154–2158.
[15] Y.S. Torisawa, A. Takagi, Y. Nashimoto, T. Yasukawa, H. Shiku, T. Matsue, Biomaterials 28 (2007) 559–566.
[16] H. Kimura, T. Yamamoto, H. Sakai, Y. Sakai, T. Fujii, Lab Chip 8 (2008) 741–746.
[17] T. Kaya, K. Nagamine, N. Matsui, T. Yasukawa, H. Shiku, T. Matsue, Chem. Commun. (2004) 248–249.
[18] K. Nagamine, N. Matsui, T. Kaya, T. Yasukawa, H. Shiku, T. Nakayama, T. Nishino, T. Matsue, Biosens. Bioelectron. 21 (2005) 145–151.
[19] S. Kasai, H. Shiku, Y.S. Torisawa, H. Noda, J. Yoshitake, T. Shiraishi, T. Yasukawa, T. Watanabe, T. Matsue, T. Yoshimura, Anal. Chim. Acta 549 (2005) 14–19.
[20] M. Suzuki, T. Yasukawa, H. Shiku, T. Matsue, Biosens. Bioelectron. 24 (2008) 1043–1047, doi:10.1016/j.bios.2008.06.051.
[21] T. Yasukawa, K. Nagamine, Y. Horiguchi, H. Shiku, M. Koide, T. Itayama, F. Shiraishi, T. Matsue, Anal. Chem. 80 (2008) 3722–3727.
[22] H. Shiku, S. Goto, S. Jung, K. Nagamine, M. Koide, T. Itayama, T. Yasukawa, T. Matsue, Analyst 134 (2009) 182–187.
[23] Y. Torisawa, H. Shiku, T. Yasukawa, M. Nishizawa, T. Matsue, Biomaterials 26 (2005) 2165–2172.
[24] K. Nagamine, S. Onodera, Y. Torisawa, T. Yasukawa, H. Shiku, T. Matsue, Anal. Chem. 77 (2005) 4278–4281.
[25] Y.S. Torisawa, Y. Nashimoro, T. Yasukawa, H. Shiku, T. Matsue, Biotechnol. Bioeng. 97 (2007) 615–621.
[26] N. Matsui, T. Kaya, K. Nagamine, T. Yasukawa, H. Shiku, T. Matsue, Biosens. Bioelectron. 21 (2006) 1202–1209.
[27] A. Folch, B.-H Jo, O. Hurtado, D.J. Beebe, M. Toner, J. Biomed. Mater. Res. 52 (2000) 346–353.
[28] A. Tourovskaia, T. Barber, B.T. Wickes, D. Hirdes, B. Grin, D.G. Castner, K.E. Healy, A. Folch, Langmuir 19 (2003) 4754–4764.
[29] D. Wright, B. Rajalingam, S. Selvarasah, M.R. Dokmeci, A. Khademhosseini, Lab Chip 7 (2007) 1272–1279.
[30] S. Jinno, H.-C. Moeller, C.-L. Chen, B. Rajalingam, B.G. Chung, M.R. Dokmeci, A. Khademhosseini, J. Biomed. Mater. Res. A 86 (2008) 278–288.
[31] L.H. DeRiemer, C.F. Meares, Biochemistry 20 (1981) 1606–1612.
[32] R.Q. Thompson, G.C. Barone III, H.B. Halsall, W.R. Heineman, Anal. Biochem. 192 (1991) 90–95.
[33] C.-C. Wu, T. Yasukawa, H. Shiku, T. Matsue, Sens. Actuators B 110 (2005) 342–349.
[34] Y. Takahashi, T. Miyamoto, H. Shiku, R. Asano, T. Yasukawa, I. Kumagai, T. Matsue, Anal. Chem. 81 (2009) 2785–2790.
[35] G. Wittstock, M. Burchardt, S.E. Pust, Y. Shen, C. Zhao, Angew. Chem. Int. Ed. 46 (2007) 1584–1617.
[36] A. Kelly, H. Bowen, Y.-K. Jee, N. Mahfiche, C. Soh, T. Lee, C. Hawrylowicz, P. Lavender, J. Allergy Clin. Immunol. 121 (2008) 203–208.
[37] T. Mori, F. Saito, T. Yoshino, H. Takeyama, T. Matsunaga, Biotechnol. Bioeng. 99 (2008) 1453–1461.
[38] R. Trevisan, L. Daprai, L. Paloschi, N. Vajente, L. Chieco-Bianchi, D. Saggioro, Exp. Cell Res. 312 (2006) 1390–1400.
[39] I. Tattoli, L.A. Carnerio, M. Jehanno, J.G. Magalhaes, Y. Shu, D.J. Philpott, D. Arnoult, S.E. Girardin, EMBO Rep. 9 (2008) 293–300.

Anal. Chem. **2009**, *81*, 2785–2790

Electrochemical Detection of Epidermal Growth Factor Receptors on a Single Living Cell Surface by Scanning Electrochemical Microscopy

Yasufumi Takahashi,[†] Takeshi Miyamoto,[†] Hitoshi Shiku,*[,†] Ryutaro Asano,[‡] Tomoyuki Yasukawa,[§] Izumi Kumagai,[‡] and Tomokazu Matsue*[,†]

Graduate School of Environmental Studies, Tohoku University, Aramaki Aoba 6-6-11-605, Sendai 980-8579, Japan, Graduate School of Engineering Studies, Tohoku University, Aramaki, Aoba 6-6-11-607, Sendai 980-8579, Japan, and Graduate School of Material Science, University of Hyogo, 3-2-1 Kouto, Kamigori-cho, Ako-gun, Hyogo 678-1297, Japan

A membrane protein on the surface of a single living mammalian cell was imaged by scanning electrochemical microscopy (SECM). The epidermal growth factor receptor (EGFR) is one of the key membrane proteins associated with cancer. It elicits a wide range of cell-type-specific responses, leading to cell proliferation, differentiation, apoptosis, and migration. To estimate EGFR expression levels by SECM, EGFR was labeled with alkaline phosphatase (ALP) via an antibody. The oxidation current of PAP (*p*-aminophenol) produced by the ALP-catalyzed reaction was monitored to estimate the density of cell surface EGFR. EGFR measurement by SECM has three advantages. First, a single adhesion cell can be measured without peeling it from the culture dish; second, it is possible to optimize labeling antibody concentrations by using living cells because detection of faradaic current is suitable for quantitative estimation in situ; and third, SECM measurements afford information on the expression state at the cell membrane at the single-cell level. In this study, we optimized the concentration of labeling antibody for EGFR at the cell surface and confirmed distinct differences in EGFR expression levels among three types of cells. SECM measurements were compatible with the results of flow cytometry.

Most membrane proteins function via intermolecular interactions. The epidermal growth factor receptor (EGFR), one of the typical membrane proteins associated with cancer, elicits a wide range of cell-type-specific responses, leading to cell proliferation, differentiation, apoptosis, and migration.[1−3] Since EGFR can trigger irregular cellular proliferation, it has been considered an attractive target molecule for cancer therapy.[4,5] Various methods have been introduced to study EGFR. These methods can be categorized into three main approaches. The first approach uses fluorescent measurement to clarify cellular signaling induced by EGFR. Dimerization of EGF−EGFR complexes and autophosphorylation of EGFR have been visualized by total internal reflection fluorescence microscopy.[6] In addition, fluorescence resonance energy transfer (FRET) imaging has been used to monitor the morphological changes induced by EGF stimulation.[7−9] In a microfluidic system where it is possible to induce local stimulation, laminar flows containing fluorescent-labeled EGF have revealed lateral propagation of EGFR signaling on single living cell surfaces.[10] The second approach examines EGFR as a target molecule for cancer therapy. The anti-EGFR antibody cetuximab, which is used for treatment of metastatic cancers of the colon, head, and neck, is known to prevent receptor activation, thus blocking downstream signaling.[4] The third approach involves the measurement of EGFR density and its distribution on cell surfaces. Radioisotope labeling,[11] fluorescent labeling,[12] and nanoparticle labeling[13,14] have been performed in order to estimate or image the expression level of EGFR. After stimulation of EGF, scanning near-field optical microscopy could reveal the EGFR distribution and estimate the EGFR cluster size.[15] Flow cytometry is one of the most useful systems for estimating the membrane protein expression level.[16] However, in flow cytometric measurements, cells need to be peeled off from the culture dish bottom; this process has the potential to cause unexpected changes in the state

* To whom correspondence should be addressed. Phone and fax: +81-22-795-7209. E-mail: shiku@bioinfo.che.tohoku.ac.jp (H.S.); matsue@bioinfo.che.tohoku.ac.jp (T.M.).

† Graduate School of Environmental Studies, Tohoku University.

‡ Graduate School of Engineering Studies, Tohoku University.

§ University of Hyogo.

(1) Ullrich, A.; Schlessingert, J. *Cell* **1990**, *61*, 203–212.
(2) Jaiswal, J. K.; Simon, S. M. *Nat. Chem. Biol.* **2007**, *3*, 92–98.
(3) Ishii, Y.; Yanagida, T. *Single Mol.* **2000**, *1*, 5–16.
(4) Ciardiello, F.; Tortora, G. *Clin. Cancer Res.* **2001**, *7*, 2958–2970.
(5) Asano, R.; Sone, Y.; Ikoma, K.; Hayashi, H.; Nakanishi, T.; Umetsu, M.; Katayose, Y.; Unno, M.; Kudo, T.; Kumagai, I. *Protein Eng.* **2008**, *21*, 597–603.
(6) Sako, Y.; Minoguchi, S.; Yanagida, T. *Nat. Cell Biol.* **2000**, *2*, 168–172.
(7) Clayton, A. H. A.; Tavarnesi, M. L.; Johns, T. G. *Biochemistry* **2007**, *46*, 4589–4597.
(8) Gadella, T. W. J.; Jovin, T. M., Jr. *J. Cell Biol.* **1995**, *129*, 1543–1558.
(9) Sorkin, A.; McClure, M.; Huang, F.; Carter, R. *Curr. Biol.* **2000**, *10*, 1395–1398.
(10) Sawano, A.; Takayama, S.; Matsuda, M.; Miyawaki, A. *Dev. Cell* **2002**, *3*, 245–257.
(11) Wrann, M. M.; Fox, C. F. *Bio. Chem.* **1979**, *254*, 8083–8086.
(12) Liu, W.; Howarth, M.; Greytak, A. B.; Zheng, Y.; Nocera, D. G.; Ting, A. Y.; Bawendi, M. G. *J. Am. Chem. Soc.* **2008**, *130*, 1274–1284.
(13) El-Sayed, I. H.; Huang, X.; El-Sayed, M. A. *Nano Lett.* **2005**, *5*, 829–834.
(14) Huang, X.; El-Sayed, I. H.; Qian, W.; El-Sayed, M. A. *J. Am. Chem. Soc.* **2006**, *128*, 2115–2120.
(15) Nagy, P.; Jenei, A.; Kirsch, A. K.; Szöllösi, J.; Damjanovich, S.; Jovin, T. M. *J. Cell Sci.* **1999**, *112*, 1733–1741.
(16) Kimmig, R.; Pfeiffer, D.; Landsmann, H.; Hepp, H. *Int. J. Cancer* **1997**, *74*, 365–373.

10.1021/ac900195m CCC: $40.75 © 2009 American Chemical Society
Published on Web 03/05/2009

of the cell surface. Fluorescent microscopy allows adhesion cell measurement, but it is not suitable for quantitative analysis because of photobleaching and autofluorescence of the cell itself.

Scanning electrochemical microscopy (SECM) has been successfully used to investigate various biological systems. This is because a localized chemical reaction under physiological conditions can be quantitatively characterized in situ in a noninvasive manner.[17−22] While in most analytical tools, the sample must be physically attached to the sensor, a feature of the SECM is the ability to set the detector, namely, the microelectrode, near the sample surface. Therefore, living cell measurement can be carried out in situ by SECM. We have previously developed SECM-based enzyme-linked immunosorbent assays (ELISA) for detecting antigen[23−27] and cytokine[28] molecules by using the sandwich methodology. Wittstock et al. reported on the characterization of antibodies immobilized on magnetic beads in order to improve the sample preparation of beads and sensitivity of ELISA.[29,30]

With the use of enzyme-labeled antibodies, it is possible to visualize receptor proteins on the living cell membrane for SECM measurement. Membrane protein measurement by SECM has three advantages. First, a single adherent cell can be measured without peeling it from the culture dish; second, optimization of the labeling antibody concentration is possible because faradaic current is suitable for quantitative estimation; and third, a faradaic current image corresponding to the expression state of the measured membrane protein is available at the single-cell level. However, there have been no reports in the literature on the application of SECM to membrane protein measurement. The current study is the first to use SECM to measure membrane protein.

EXPERIMENTAL SECTION

Chemicals. The primary antibodies (mouse anti-EGFR IgG [sc-120, Santa Cruz Biotechnology, Santa Cruz, CA], mouse anti-EGFR IgG FITC conjugated [sc-120 FITC, Santa Cruz Biotechnology, Santa Cruz, CA]), the secondary antibodies (alkaline phosphatase [ALP]-goat antimouse IgG [62−6522, Zymed], β-galactosidase[β-Gal]-goat antimouse IgG [A-106GN, American Qual-ex]), Diaphorase-1 (Dp, *Bacillus stearothermophilus*; Unitika Ltd.), NADH (Calzyme Laboratories, Inc.), a Biotin Labeling kit-NH_2 (Dojindo Laboratory), *p*-aminophenylphosphate monosodium salt (PAPP; LKT Laboratory Inc.), *p*-aminophenol (PAP; Wako Pure Chemical Industries), *p*-aminophenyl-β-D-galactopyranoside (PAPG; Wako Pure Chemical Industries), ferrocenemethanol ($FcCH_2OH$; Aldrich), and poly(dimethylsiloxane) (PDMS; Dow Corning Toray Co., Ltd.) were purchased and used as received. All other chemicals were used as received. All the solutions were prepared using distilled water obtained from a Milli-Q (Millipore, Japan).

Cell Culture. A normal Chinese hamster ovary (CHO) and cells derived from human epidermoid carcinoma cell line A431 were donated from the Cell Resource Center for Biomedical Research (Tohoku University). The EGFR/CHO (CHO transfected with EGFR) used in this study were prepared according to the literature.[5]

Normal CHO and A431 cells were cultured in an RPMI-1640 medium (Gibco Invitrogen, Tokyo, Japan) containing 10% fetal bovine serum (FBS; Gibco), 50 μg/mL penicillin (Gibco), and 50 μg/mL streptomycin (Gibco) at 37 °C in a humidified atmosphere containing 5% CO_2. The EGFR/CHO cells were cultured in RPMI-1640 medium (Sigma) containing 10% fetal bovine serum (FBS, Gibco), 50 μg/mL G418 (Nacalai Tesque) at 37 °C in a humidified atmosphere containing 5% CO_2.

Labeling EGFR with Enzymes via Antibodies. EGFR was labeled with ALP, β-Gal, or Dp via antibodies for electrochemical detection. For ALP labeling, the cells were incubated for 90 min in RPMI-1640 with anti-EGFR antibody (1 μg/mL), followed by thorough washing with RPMI-1640. Cells were then incubated for 90 min in RPMI-1640 with ALP-labeled secondary antibody (1 μg/mL). EGFR was also labeled with β-Gal using the same procedure as that used for ALP labeling.

For labeling with Dp, the cells were incubated for 60 min in RPMI-1640 with a biotin-labeled anti-EGFR antibody (1 μg/mL, 100 μL). After thorough washing with phosphate buffered saline (PBS), the cells were incubated for 30 min in RPMI-1640 containing bovine serum albumin (BSA, 10 mg/mL) to block physical adsorption of interfering proteins. The cells were then incubated for 30 min in RPMI-1640 with avidin (10 mg/mL). After extensive washing with PBS, the cells were treated in RPMI-1640 with biotin-labeled Dp (25 μg/mL) for 40 min. Biotinylation of anti-EGFR antibody and Dp was carried out using a Biotin Labeling kit-NH_2.

SECM Measurements. We used two EGFR-detection methods for SECM measurements, the substrate generation/tip collection mode and the feedback mode (Figure 1). The measurements were conducted using a HEPES-based saline solution (10 mM HEPES, 150 mM NaCl, 4.2 mM KCl, and 11.2 mM glucose; pH 9.5) containing 4.7 mM PAPP and 10% FBS for detection of ALP-labeled EGFR. HEPES-based saline solution (pH 7.5) containing 7.4 mM PAPG was used for the detection of β-Gal-labeled EGFR, and HEPES-based saline solution (pH 7.5) containing 0.5 mM $FcCH_2OH$ was used for Dp-labeled EGFR.

The potential of the microelectrode probe was set at +0.30 V vs Ag/AgCl for the detection of ALP- and β-Gal-labeled EGFR. ALP and β-Gal catalyzed the hydrolysis of PAPP and PAPG, respectively. Both enzyme reactions yielded PAP as an enzymatic

(17) Shiku, H.; Shiraishi, T.; Ohya, H.; Matsue, T.; Abe, H.; Hoshi, H.; Kobayashi, M. *Anal. Chem.* **2001**, *73*, 3751–3758.
(18) Torisawa, Y.; Ohara, N.; Nagamine, K.; Kasai, S.; Yasukawa, T.; Shiku, H.; Matsue, T. *Anal. Chem.* **2006**, *78*, 7625–7631.
(19) Bard, A. J.; Li, X.; Zhan, W. *Biosens. Bioelectron.* **2006**, *22*, 461–472.
(20) Amemiya, S.; Guo, J.; Xiong, H.; Gross, D. A. *Anal. Bioanal. Chem.* **2006**, *386*, 458–471.
(21) Schulte, A.; Schuhmann, W. *Angew. Chem., Int. Ed.* **2007**, *46*, 2–20.
(22) Wittstock, G.; Burchardt, M.; Pust, S. E.; Shen, Y.; Zhao, C. *Angew. Chem., Int. Ed.* **2007**, *46*, 1584–1617.
(23) Shiku, H.; Matsue, T.; Uchida, I. *Anal. Chem.* **1996**, *68*, 1276–1278.
(24) Wittstock, G.; Yu, K.; Halsall, H. B.; Ridgway, T. H.; Heineman, W. R. *Anal. Chem.* **1995**, *67*, 3578–3582.
(25) Shiku, H.; Hara, Y.; Matsue, T.; Uchida, I.; Yamauchi, T. *J. Electroanal. Chem.* **1997**, *438*, 187–190.
(26) Kasai, S.; Yokota, A.; Zhou, H.; Nishizawa, M.; Niwa, K.; Onouchi, T.; Matsue, T. *Anal. Chem.* **2000**, *72*, 5761–5765.
(27) Yasukawa, T.; Hirano, Y.; Motochi, N.; Shiku, H.; Matsue, T. *Biosens. Bioelectron.* **2007**, *22*, 3099–3104.
(28) Kasai, S.; Shiku, H.; Torisawa, Y.; Nagamine, K.; Yasukawa, T.; Watanabe, T.; Matsue, T. *Anal. Chim. Acta* **2006**, *566*, 55–59.
(29) Wijayawardhana, C. A.; Wittstock, G.; Halsall, H. B.; Heineman, W. R. *Anal. Chem.* **2000**, *72*, 333–338.
(30) Wijayawardhana, C. A.; Wittstock, G.; Halsall, H. B.; Heineman, W. R. *Electroanalysis* **2000**, *12*, 640–644.

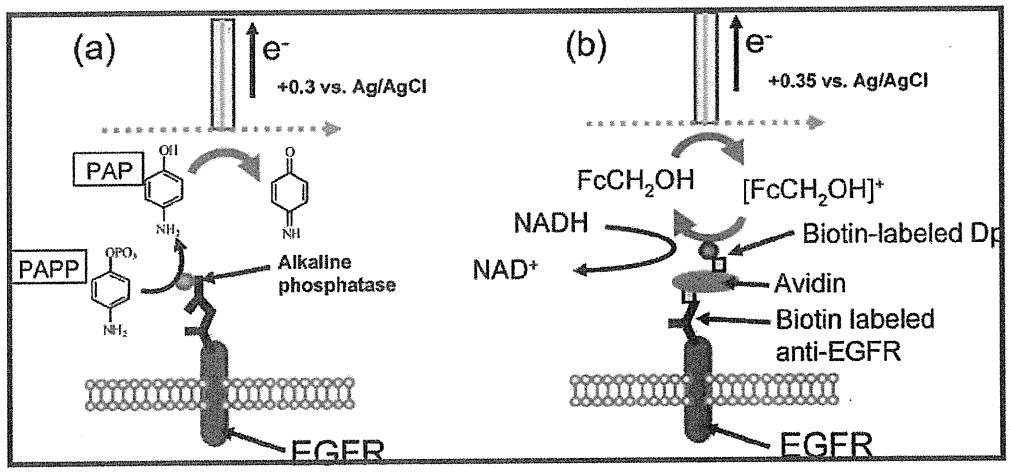

Figure 1. Schematic diagrams of EGFR detection using (a) generation-collection mode and (b) feedback mode.

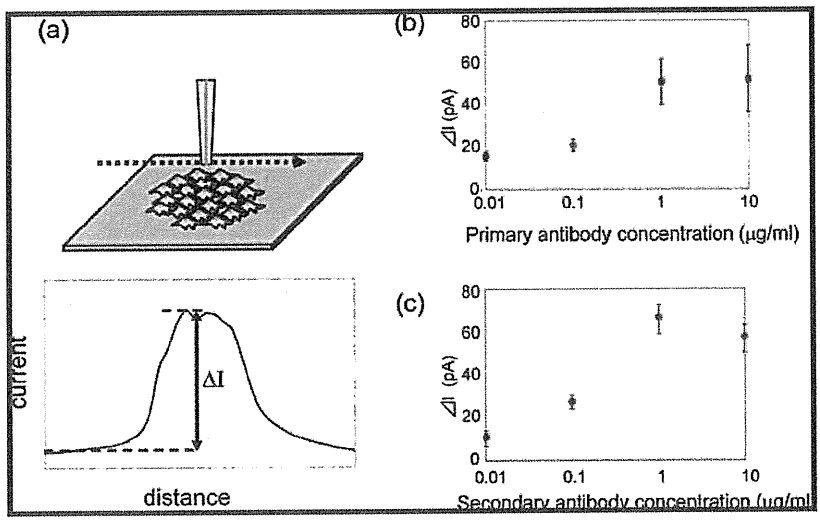

Figure 2. Optimization of antibody concentration. (a) Schematic representation of standardization of current ΔI. Oxidation current response as a function of the (b) primary antibody concentration (secondary antibody concentration is 1 μg/ml) and (c) secondary antibody concentration (primary antibody concentration is 10 μg/ml). The electrode was set at 20 μm above the substrate, and the scan rate was 10 μm/s.

product, which was detected electrochemically at the microelectrode probe of SECM set at +0.30 V vs Ag/AgCl (Figure 1a). In the case of Dp labeling, the potential of the probe was set at +0.35 V vs Ag/AgCl to oxidize $FcCH_2OH$ to $[FcCH_2OH]^+$, which was reduced again to $FcCH_2OH$ by the Dp-catalyzed reaction at the membrane surface in the presence of NADH. This enzymatic regeneration of $FcCH_2OH$ increased the oxidation current at the probe (Figure 1b).

A disk-type platinum electrode with a 20 μm diameter was used as a SECM microelectrode probe and as a working electrode. Electrochemical current was measured on the basis of a two-electrode configuration using an Ag/AgCl electrode as the reference electrode. The current was amplified with a current amplifier (428, Keithley). Movement of the microelectrode tip was performed by a motor-driven *XYZ* stage (K701-20RMS, Suruga Seiki) and a stage controller (D70, Suruga Seiki). The details of the SECM system were reported previously.[18]

Preparation of the Cell-Patterned Substrate. For the estimation of EGFR expression levels, a flat substrate patterned with approximately 300 cells was fabricated by the PDMS microstenciling method. The microstencil was a 100 μm-thick PDMS sheet with a 3 × 3 array of 300 μm diameter circles, prepared using a CO_2 laser beam (Universal Laser Systems, Scottsdale, Arizona). The cells (10^6 cells/mL, 100 μL) were seeded on a 35 mm dish (Falcon), sealed with the PDMS microstencil, and incubated for 2 h to allow the cells to adhere to the dish. The excess nonadherent cells were then removed by washing with RPMI-1640. After incubation for 1 day in RPMI-1640, the stencil was peeled off from the dish and the SECM measurement was performed (Figure 2a).

RESULTS AND DISCUSSION

Because the SECM is sensitive to the diffusion and permeation of chemicals, SECM measurements can distinguish whether a chemical reagent is derived from the outside or inside of the cell

(31) Matsue, T.; Shiku, H.; Yamada, H.; Uchida, I. *J. Phys. Chem.* 1994, *98*, 11001–11003.
(32) Wilburn, J. P.; Wright, D. W.; Cliffel, D. E. *Analyst* 2006, *131*, 311–316.
(33) Sun, P.; Laforge, F. O.; Abeyweera, T. P.; Rotenberg, S. A.; Carpino, J.; Mirkin, M. V. *Proc. Natl. Acad. Sci. U.S.A.* 2008, *105*, 443–448.
(34) Feng, W.; Rotenberg, S. A.; Mirkin, M. V. *Anal. Chem.* 2003, *75*, 4148–4154.
(35) Zhan, W.; Bard, A. J. *Anal. Chem.* 2006, *78*, 726–733.

membrane.[19,31–35] Furthermore, real-time monitoring of cell surface phenomena, including endocytosis and exocytosis,[21,36–39] is also possible. In this study, we optimized the concentration of the primary and secondary antibodies for EGFR labeling. We used three types of cells: normal CHO without EGFR, EGFR/CHO expressing EGFR, and A431 originally expressing EGFR with very high density. The current response that originated from ALP-labeled EGFR at the cell membranes was measured with the SECM in a HEPES-based saline solution of pH 9.5. During the measurements, the cells were alive for at least 3 h in the solution, although it is important to consider the toxicity of the enzyme substrate and the product. The results were compared with those from flow cytometry (see Supporting Information).

Optimization of Antibody Concentration by SECM Measurements. The binding ability of the ALP antibody to EGFR was estimated from the PAP oxidation current produced by the ALP-catalyzed reaction at the cell surfaces. The PAP oxidation was measured by a single-scan measurement above a circular cell pattern comprising approximately 300 EGFR/CHO cells. Larger oxidation currents were observed when the microelectrode probe scanned over the cell pattern. The peak response, observed at the center of the pattern (Figure 2a), increased as the primary or secondary antibody concentration for ALP labeling of EGFR increased (Figure 2b,c). On the basis of these results, in subsequent measurements, the concentrations of both the primary and secondary antibodies were set at 1 μg/mL.

Investigation of CHO Cells Using β-Gal or Dp as a Labeling Enzyme with SECM. We also used β-Gal as an EGFR-labeling enzyme because β-Gal functions in neutral pH. Figure 3 shows the current responses obtained by a single-scan measurement with the SECM substrate generation/tip collection mode for the cell patterns of β-Gal-labeled EGFR/CHO cells and nonlabeled EGFR/CHO cells. The current responses of EGFR/CHO cells were found to be less than 3 pA, which was 1 order of magnitude smaller than that found for ALP-labeled cells. Therefore, we concluded that β-Gal is not suitable for single-cell imaging since single-cell imaging requires a highly active enzyme to detect a small number of EGFRs. However, it should be noted that β-Gal labeling minimized the background current, as evident by the fact that no response was observed for the nonlabeled EGFR/CHO cells. Usually, mammalian cells naturally have no endogenous galactosidase, whereas ALP is widely expressed in various types of cells.

As another labeling enzyme functioning in neutral pH, diaphorase (Dp) would be applicable in feedback-mode SECM. In this measurement mode, the probe electrode was set at +0.35 V to oxidize $FcCH_2OH$ to $[FcCH_2OH]^+$, which was reduced again to $FcCH_2OH$ by the Dp-catalyzed reaction at the cell membrane in the presence of NADH. This redox cycling generated additional oxidation current for $FcCH_2OH$. Figure 4 shows the SECM images of the patterned cell with Dp-labeled EGFR/CHO in the presence and absence of NADH. The addition of NADH

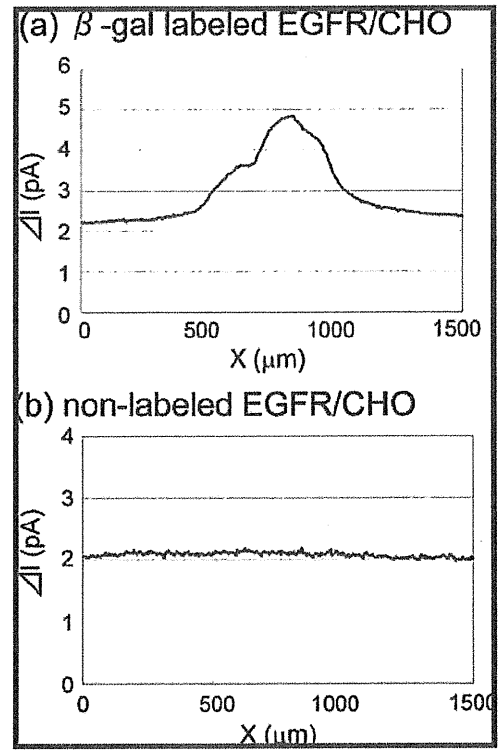

Figure 3. One-line scan of microstencil-patterned cells (a) β-gal-labeled EGFR/CHO and (b) nonlabeled EGFR/CHO in substrate generation/tip collection mode SECM. The electrode was set at 20 μm above the substrate, and the scan rate was 10 μm/s. The scan range was 1500 μm.

significantly increased the current responses, indicating that Dp can also be used as a labeling enzyme for imaging EGFR/CHO cells. The small current response prior to adding NADH was probably caused by intracellular reduction of $[FcCH_2OH]^+$ as it permeated through the cell membrane (see Supporting Information). In addition, we found that the current response for EGFR/CHO cells without enzyme labeling depends on the tip scan rate. This could be also because the $FcCH_2OH$ penetrates the cell, and the tip electrode exhausts the redox inside the cell at a very slow scan rate. Similar problems occur when probing redox active thin-layer systems.[40–43]

SECM Images of EGFR at the Cell Surface of a Single Living Cell. Figure 5 shows single-cell imaging with the SECM substrate generation/tip collection mode for EGFR/CHO and normal CHO. ALP was selected as the labeling enzyme. The current response of the EGFR/CHO cell was considerably larger than that of normal CHO. This result indicated that SECM can distinguish the EGFR expression level of a single adhesion cell without peeling it from the dish. To our knowledge, there have been no other reports on the detection of specific proteins at the cell surface by using SECM-based ELISA, although SECM-based

(36) Liebetrau, J. M.; Miller, H. M.; Baur, J. E.; Takacs, S. A.; Anupunpisit, V.; Garris, P. A.; Wipf, D. O. *Anal. Chem.* 2003, *75*, 563–571.
(37) Ciolkowski, E. L.; Cooper, B. R.; Jankowski, J. A.; Jorgenson, J. W.; Wightman, R. M. *J. Am. Chem. Soc.* 1992, *114*, 2815–2821.
(38) Hengstenberg, A.; Blöchl, A.; Dietzel, I. D.; Schuhmann, W. *Angew. Chem., Int. Ed.* 2001, *40*, 905–908.
(39) Kurulugama, R. T.; Wipf, D. O.; Takacs, S. A.; Pongmayteegul, S.; Garris, P. A.; Baur, J. E. *Anal. Chem.* 2005, *77*, 1111–1117.
(40) Zhang, J.; Slevin, C. J.; Morton, C.; Scott, P.; Walton, D. J.; Unwin, P. R. *J. Phys. Chem. B* 2001, *105*, 11120–11130.
(41) O'Mullane, A. P.; Macpherson, J. V.; Unwin, P. R.; Cervera-Mopntesinos, J.; Manzanares, J. A.; Frehill, F.; Vos, J. G. *J. Phys. Chem. B* 2004, *108*, 7219–7227.
(42) Nijhuis, C. A.; Sinha, K. K.; Wittstock, G.; Huskens, J.; Ravoo, B. J.; Reinhoudt, D. N. *Langmuir* 2006, *22*, 9770–9775.
(43) Zhang, M.; Wittstock, G.; Shao, Y.; Girault, H. H. *Anal. Chem.* 2007, *79*, 4833–4839.

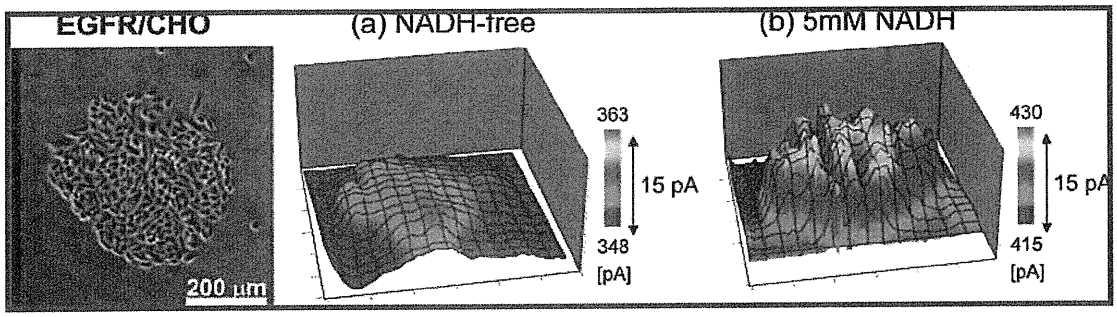

Figure 4. SECM feedback mode image of microstencil-patterned EGFR/CHO cells. EGFR/CHO cells imaged in the NADH-free solution and in 5 mM NADH solution. The electrode was set at 15 μm above the substrate, and the scan rate was 50 μm/s. The scan range was 600 μm × 600 μm, and the step size was 10 μm.

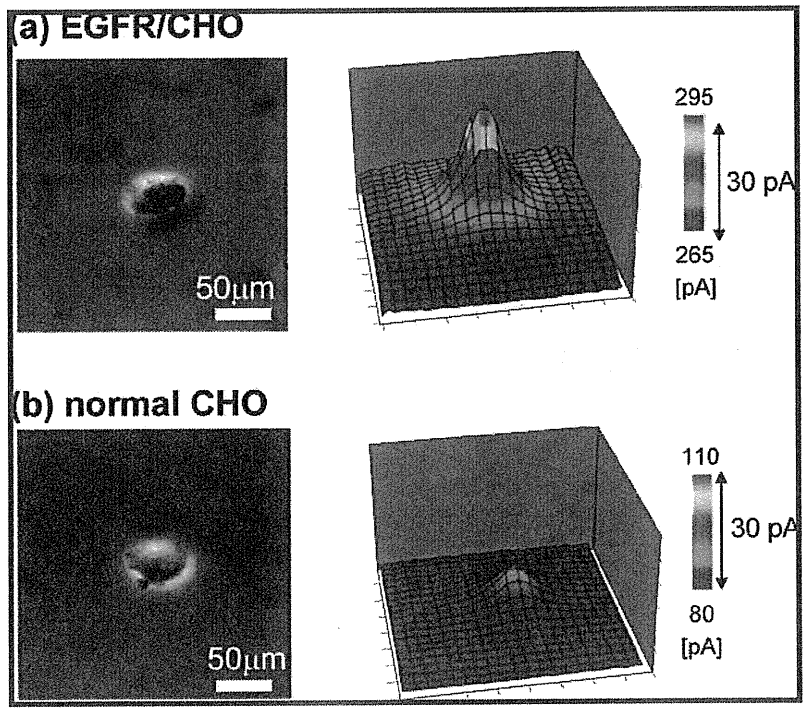

Figure 5. Single CHO cell SECM image in substrate generation/tip collection mode: (a) EGFR/CHO cell and (b) normal CHO cell. The electrode was set at 15 μm above the substrate, and the scan rate was 5 μm/s. The scan range was 200 μm × 200 μm, and the step size was 5 μm.

ELISA has been applied to detect antigens[23–27] and cytokines[28] on solid surfaces. The present study is the first to demonstrate SECM measurement of a cell membrane protein at the single-cell level.

Mammalians cells naturally show endogenous phosphatase activity that is significant in the context of SECM imaging at the single-cell level. Therefore, we corrected the EGFR expression signal by subtracting the current response of nonlabeled cells from that of ALP-labeled cells in a single-scan measurement. The peak currents of nonlabeled normal CHO, EGFR/CHO, and A431 cells were 7.9 ± 6.0 pA (n = 5), 5.4 ± 2.5 pA (n = 3), and 6.8 ± 0.8 pA (n = 8), respectively. These responses were considered background signals and subtracted from the current responses for ALP-labeled cells. Figure 6 shows the peak currents for ALP-labeled cells after subtraction. Significant differences were found in the responses for the three types of cells as follows: CHO < EGFR/CHO < A431 (p < 0.001, normal CHO and EGFR/CHO; p < 0.060, EGFR/CHO and A431). The same order of EGFR expression levels was also found in measurements by flow cytometry (see Supporting Information, Figure S1). The expression level for EGFR/CHO relative to that for A431 was 0.33, which was the same as that determined by flow cytometry. This agreement reinforces the conclusion that SECM measurement provides a reliable estimation of the EGFR expression levels. It should be noted that SECM provides quantitative, continuous information on single

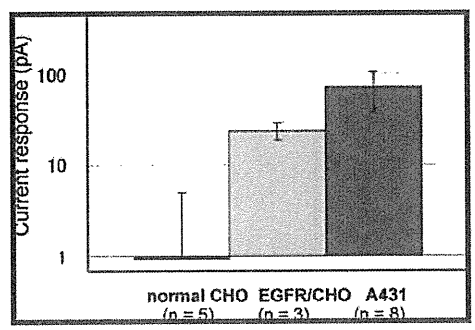

Figure 6. Relative EGFR expression level of a single cell measured by SECM in substrate generation/tip collection mode.

living, single adherent cells without peeling them from the dish. In the future, the mapping of EGFR on the cell surface and the real-time monitoring of endocytosis induced by EGF stimulation will also be possible.

CONCLUSION

In this study, we have described the membrane protein imaging of living cells with SECM. The expression level of EGFR at the cell surface of an adherent single cell was measured without peeling it from the culture dish by using enzyme-labeled antibodies. Furthermore, imaging at the single-cell level was successfully performed, demonstrating that the expression level is statically distinguishable in the following descending order: normal CHO, EGFR/CHO, and A431.

The formation of the EGF–EGFR complex triggers endocytosis and subsequent cell proliferation. Thus, real-time monitoring of EGFR density at the cell membrane affords quantitative information about the initial stage of cell signaling. Unlike fluorescence imaging, the SECM procedure described in the present study is, in principle, surface sensitive; therefore, it is advantageous in selectively detecting the processes occurring at the outer membrane surface. We think that SECM measurement is particularly suitable for monitoring EGF-triggered endocytosis, in which EGF induces entrapment of EGFR at the cell surface into the inside of the cell. Furthermore, because SECM is a versatile system that can be used not only for quantitative membrane analysis but also for topographic or optical imaging[44] of cells and sample manipulation (including simultaneous injection/collection of biomolecules[45]), other membrane protein-related phenomena could also be continuously and successfully monitored by SECM.

ACKNOWLEDGMENT

This work was partly supported by Grants-in-Aid for Scientific Research (Grants 18101006 and 19750055) from MEXT (Ministry of Education, Culture, Sports, Science and Technology), Japan; and by a grant from the Center for Interdisciplinary Research, Tohoku University. Y.T. acknowledges the support obtained from a research fellowship of the Japan Society for the Promotion of Science. The A431 cells and normal CHO cells were donated by the Institute of Development, Aging and Cancer, Tohoku University.

SUPPORTING INFORMATION AVAILABLE

Additional information as noted in text. This material is available free of charge via the Internet at http://pubs.acs.org.

Received for review January 26, 2009. Accepted February 12, 2009.

AC900195M

(44) Takahashi, Y.; Hirano, Y.; Yasukawa, T.; Shiku, H.; Yamada, H.; Matsue, T. *Langmuir* **2006**, *22*, 10299–10306.

(45) Nashimoto, Y.; Takahashi, Y.; Yamakawa, T.; Torisawa, Y.; Yasukawa, T.; Tio-Sasaki, T.; Yokoo, M.; Abe, H.; Shiku, H.; Kambara, H.; Matsue, T. *Anal. Chem.* **2007**, *79*, 6823–6830.

Anal. Chem. 2009, *81*, 9674–9681

Transfected Single-Cell Imaging by Scanning Electrochemical Optical Microscopy with Shear Force Feedback Regulation

Yasufumi Takahashi,[†] Hitoshi Shiku,*[,†] Tatsuya Murata,[†] Tomoyuki Yasukawa,[‡] and Tomokazu Matsue*[,†]

Graduate School of Environmental Studies, Tohoku University, Aramaki Aoba 6-6-11-605, Sendai 980-8579, Japan, and Graduate School of Material Science, University of Hyogo, 3-2-1 Kouto, Kamigori-cho, Ako-gun, Hyogo 678-1297, Japan

Gene-transfected single HeLa cells were characterized using a scanning electrochemical/optical microscope (SECM/OM) system with shear-force-based probe-sample distance regulation to simultaneously capture electrochemical, fluorescent, and topographic images. The outer and inner states of single living cells were obtained as electrochemical and fluorescent signals, respectively, by using an optical fiber-nanoelectrode probe. A focused ion beam (FIB) was used to mill the optical aperture and the ring electrode at the probe apex (the inner and outer radii of the ring electrode were 37 and 112 nm, respectively). To apply an appropriate shear force between the probe tip and the living cell surface, we optimized the amplitude of oscillation of the tuning fork to which the probe was attached. Field-programmable gate arrays (FPGA) were adopted to drastically increase the feedback speed of the tip−sample distance regulation, shorten the scanning time for imaging, and enhance the accuracy and quality of the living cell images. In employing these improvements, we simultaneously measured the cellular expression activity of both secreted alkaline phosphatase outside and GFP inside by using the SECM/OM with shear force distance regulation.

Scanning electrochemical microscopy (SECM) has been successfully used to investigate various biological systems because it allows the physiological conditions of localized chemical species to be quantitatively characterized in situ in a non-invasive manner.[1−5] Significant efforts have been made to improve the electrochemical measurement sensitivity, lateral resolution, and quality of SECM by using nanoelectrodes[6−11] as scanning probes and by incorporating distance control mechanisms related to atomic force microscopy (AFM),[12−15] shear force,[16−22] faradaic current,[23−25] and impedance[26−28] to detect chemicals having very short life spans or those present in trace amounts, such as neurotransmitters,[16,23] NO,[19] and oxygen.[17] Ueda et al. observed the PC12 axons abnormally swollen topography using SECM/NSOM (near-field scanning optical microscopy)/AFM.[14] They proposed the possibility of characterizing living cells to obtain chemical information on the inner and outer states by means of electrochemical and optical measurements, receptivity studies, and

* To whom correspondence should be addressed. Phone/Fax: +81-22-795-7209. E-mail: shiku@bioinfo.che.tohoku.ac.jp (H.S.); matsue@bioinfo.che.tohoku.ac.jp (T.M.).

† Tohoku University.

‡ University of Hyogo.

(1) Bard, A. J.; Mirkin, M. V. *Scanning Electrochemical Microscopy*, 1st ed.; Marcel Dekker, Inc.: New York, 2001.
(2) Amemiya, S.; Bard, A. J.; Fan, F. R. F.; Mirkin, M. V.; Unwin, P. R. *Annu. Rev. Anal. Chem.* 2008, *1*, 95–131.
(3) Roberts, W. S.; Lonsdale, D. J.; Griffiths, J.; Higson, S. P. J. *Biosens. Bioelectron.* 2007, *23*, 301–318.
(4) Schulte, A.; Schuhmann, W. *Angew. Chem., Int. Ed.* 2007, *46*, 8760–8777.
(5) Wittstock, G.; Burchardt, M.; Pust, S. E.; Shen, Y.; Zhao, C. *Angew. Chem., Int. Ed.* 2007, *46*, 1584–1617.
(6) Shao, Y. H.; Mirkin, M. V.; Fish, G.; Kokotov, S.; Palanker, D.; Lewis, A. *Anal. Chem.* 1997, *69*, 1627–1634.
(7) Slevin, C. J.; Gray, N. J.; Macpherson, J. V.; Webb, M. A.; Unwin, P. R. *Electrochem. Commun.* 1999, *1*, 282–288.
(8) Katemann, B. B.; Schuhmann, T. *Electroanalysis* 2002, *14*, 22–28.
(9) Xiong, H.; Guo, J. D.; Kurihara, K.; Amemiya, S. *Electrochem. Commun.* 2004, *6*, 615–620.
(10) Wu, W. Z.; Huang, W. H.; Wang, W.; Wang, Z. L.; Cheng, J. K.; Xu, T.; Zhang, R. Y.; Chen, Y.; Liut, *J. Am. Chem. Soc.* 2005, *127*, 8914–8915.
(11) Ufheil, J.; Hess, C.; Borgwarth, K.; Heinze, J. *Phys. Chem. Chem. Phys.* 2005, *7*, 3185–3190.
(12) Macpherson, J. V.; Jones, C. E.; Barker, A. L.; Unwin, P. R. *Anal. Chem.* 2002, *74*, 1841–1848.
(13) Kueng, A.; Kranz, C.; Lugstein, A.; Bertagnolli, E.; Mizaikoff, B. *Angew. Chem., Int. Ed.* 2003, *42*, 3237–3240.
(14) Ueda, A.; Niwa, O.; Maruyama, K.; Shindo, Y.; Oka, K.; Suzuki, K. *Angew. Chem., Int. Ed.* 2007, *46*, 8238–8241.
(15) Zhao, X. C.; Petersen, N. O.; Ding, Z. F. *Can. J. Chem.* 2007, *85*, 175–183.
(16) Hengstenberg, A.; Blochl, A.; Dietzel, I. D.; Schuhmann, W. *Angew. Chem., Int. Ed.* 2001, *40*, 905–908.
(17) Takahashi, Y.; Hirano, Y.; Yasukawa, T.; Shiku, H.; Yamada, H.; Matsue, T. *Langmuir* 2006, *22*, 10299–10306.
(18) Lee, Y.; Ding, Z. F.; Bard, A. *J. Anal. Chem.* 2002, *74*, 3634–3643.
(19) Isik, S.; Schuhmann, W. *Angew. Chem., Int. Ed.* 2006, *45*, 7451–7454.
(20) Yamada, H.; Fukumoto, H.; Yokoyama, T.; Koike, T. *Anal. Chem.* 2005, *77*, 1785–1790.
(21) Oyamatsu, D.; Hirano, Y.; Kanaya, N.; Mase, Y.; Nishizawa, M.; Matsue, T. *Bioelectrochemistry* 2003, *60*, 115–121.
(22) Garay, M. F.; Ufheil, J.; Borgwarth, K.; Heinze, J. *Phys. Chem. Chem. Phys.* 2004, *6*, 4028–4033.
(23) Kurulugama, R. T.; Wipf, D. O.; Takacs, S. A.; Pongmayteegul, S.; Garris, P. A.; Baur, J. E. *Anal. Chem.* 2005, *77*, 1111–1117.
(24) Isik, S.; Etienne, M.; Oni, J.; Blochl, A.; Reiter, S.; Schuhmann, W. *Anal. Chem.* 2004, *76*, 6389–6394.
(25) Fan, F. R. F.; Bard, A. J. *Proc. Natl. Acad. Sci. U.S.A.* 1999, *96*, 14222–14227.
(26) Alpuche-Aviles, M. A.; Wipf, D. O. *Anal. Chem.* 2001, *73*, 4873–4881.
(27) Diakowski, P. M.; Ding, Z. F. *Phys. Chem. Chem. Phys.* 2007, *9*, 5966–5974.
(28) Osbourn, D. M.; Sanger, R. H.; Smith, P. J. S. *Anal. Chem.* 2005, *77*, 6999–7004.

10.1021/ac901796r CCC: $40.75 © 2009 American Chemical Society
Published on Web 11/02/2009